Understanding Reactivity and Assembly of Dichalcogenides: Structural, Electrostatic Potential and Topological Analyses of 3*H*-1,2-Benzodithiol-3-one and Se Analogs

Rahul Shukla,[†] Arun Dhaka,[‡] Emmanuel Aubert,[†] Vishnu Vijayakumar-Syamala,[†] Olivier Jeannin,[‡] Marc Fourmigué*,[‡] and Enrique Espinosa*,[†]

[†] *Université de Lorraine, CNRS, CRM2, F-54000 Nancy, France. E-mail: enrique.espinosa@univ-lorraine.fr*

[‡] *Université de Rennes, CNRS, ISCR (Institut des Sciences Chimiques de Rennes), UMR 6226, Campus de Beaulieu, F-35042 Rennes, France. E-mail: marc.fourmigue@univ-rennes1.fr*

Supporting Information

Section S1. Topological Analysis of $L(\mathbf{r}) = -\nabla^2\rho(\mathbf{r})$.

The topological analysis of $L(\mathbf{r}) = -\nabla^2\rho(\mathbf{r})$ brings the characteristic critical points (CPs) of the function, where its gradient vanishes. As for $\rho(\mathbf{r})$, systems at equilibrium configuration show four types of CPs in the 3D-space (n, ω), n and ω being respectively the number of non-zero curvatures along the three main directions of the distribution and the algebraic sum of their signs (n = 3 and ω = −3, −1, +1 or +3). While (3,−3) and (3,+3) CPs indicate local maxima (3D-concentration) and minima (3D-depletion) of electronic charge, (3,−1) and (3,+1) CPs are saddle points and correspond respectively to local 1D-depletion/2D-concentration and 2D-depletion/1D-concentration along the three main directions of the L-distribution. The disposition of the saddle points in the space is not only a consequence of the sites occupied by the local 3D maxima and minima, but also of the other saddle points. Thus, along 1D main direction belonging to a 2D-surface that embraces three CPs, a central (3,−1) CP can be faced by either (3,−3) or (3,+1) CPs, whereas a central (3,+1) CP can be faced by either (3,+3) or (3,−1) CPs. In all cases, the consecutive appearance of local 1D-maxima and 1D-minima is a consequence of both the finite values and the continuity of the L-function and its derivatives in the space.[1]

Charge concentration (CC) and charge depletion (CD) sites in the valence shell of atoms are associated to local nucleophilic and electrophilic atomic sites.[2] Whereas for lighter atoms (for instance, O, F, S or Cl) CC and CD sites appear in the atomic valence-shell charge concentration (VSCC) region, for heavier atoms (for instance, Se, Br, Te, or I) CC and CD sites show in the extended atomic valence-shell charge depletion (VSCD) region.[3,4] Indeed, because of the large quantity of core electrons, valence electrons follow a significant screening in heavier atoms, and therefore a huge depletion of their charge density with the concomitant VSCC shrinking (up to vanish for heavier ones).[1] As indicated in previous works,[3,4] local electrostatic electrophilic•••nucleophilic interactions between atomic CD and CC sites drive geometrical preferences in intermolecular interactions, the CD•••CC direction being very close to the internuclear direction of the involved atoms (the angle between both directions being typically less than 15°). Nucleophilic CC sites are observed in concentrated regions of the atomic valence-shells (lone pairs regions) and correspond to (3,−3) CPs in the topology of the L-function. Electrophilic CD sites are observed in depleted regions of atomic valence-shells and correspond in most cases to (3,+1) CPs in the topology of the L-function, even if in some cases (3,+3) or (3,−1) CPs can

appear instead. This is for instance the case of hydrogen atoms, where a (3,+3) CP marks in many cases the electrophilic CD site along the bonding axis. For other atoms, in the absence of a (3,+1) CP a less performer (3,−1) CP can take over the CD site (the latter behaving as a 1D-depletion site in front of the 2D-depletion site for the former).

Because the $L(\mathbf{r}) = -\nabla^2\rho(\mathbf{r})$ distribution exhibits positive and negative values, and varies rapidly in the space, the topology of $L(\mathbf{r})$ is difficult to interpret. In particular, many CPs of all types exhibit around atoms and care should be taken in the selection of the relevant ones for discussions. To this respect, it has been shown that only CPs laying on (or very close to) interaction planes and belonging to VSCC (for lighter atoms) or VSCD (for heavier atoms) are mostly relevant.[1,3,4] In this work, we will extend these criteria to focus on selected CPs belonging to chalcogen atoms.

The electrophilic/nucleophilic power of CD/CC sites can be monitored by the L/ρ value at the corresponding sites (the normalization by ρ permitting the comparison between atoms with a different number of electrons). Thus, the larger the positive/negative L/ρ magnitude the more nucleophilic/electrophilic power of the site. Accordingly, the larger the positive difference $\Delta(L/\rho) = (L/\rho)_{CC} - (L/\rho)_{CD}$ the more important is the nucleophilic•••electrophilic interaction. In the interaction of electrophilic and nucleophilic sites with their environment, we assume an inverse-square law with the distance, which corresponds to the expected geometric dilution of a point-source radiation into three-dimensional space. Hence, with the aim to monitor the intensity of the electrophilic•••nucleophilic interaction in this work we introduce the descriptor $\Delta(L/\rho)/d^2_{CD\cdots CC} = [(L/\rho)_{CC} - (L/\rho)_{CD}]/d^2_{CD\cdots CC}$, where $d^2_{CD\cdots CC}$ is the CD•••CC distance. The descriptor increases with the electrophilic and the nucleophilic power of the sites and with shorter distances. Therefore, the larger is the positive value of $\Delta(L/\rho)/d^2_{CD\cdots CC}$ the most relevant is the interaction. Thanks to the normalization per charge density unit, the descriptor permits to compare in the same scale interactions involving different kind of atoms.

The iso-surface $\nabla^2\rho(\mathbf{r}) = 0$ has been defined as the reactivity surface of molecules following a nucleophilic attack.[2] Hence, the holes observed in the surface mark the regions through which the attack can take place. In some cases, the iso-surface $\nabla^2\rho(\mathbf{r}) = 0$ does not present a hole, but appears just closing a very thin VSCC region. This is typically the case of sigma-holes in lighter atoms.

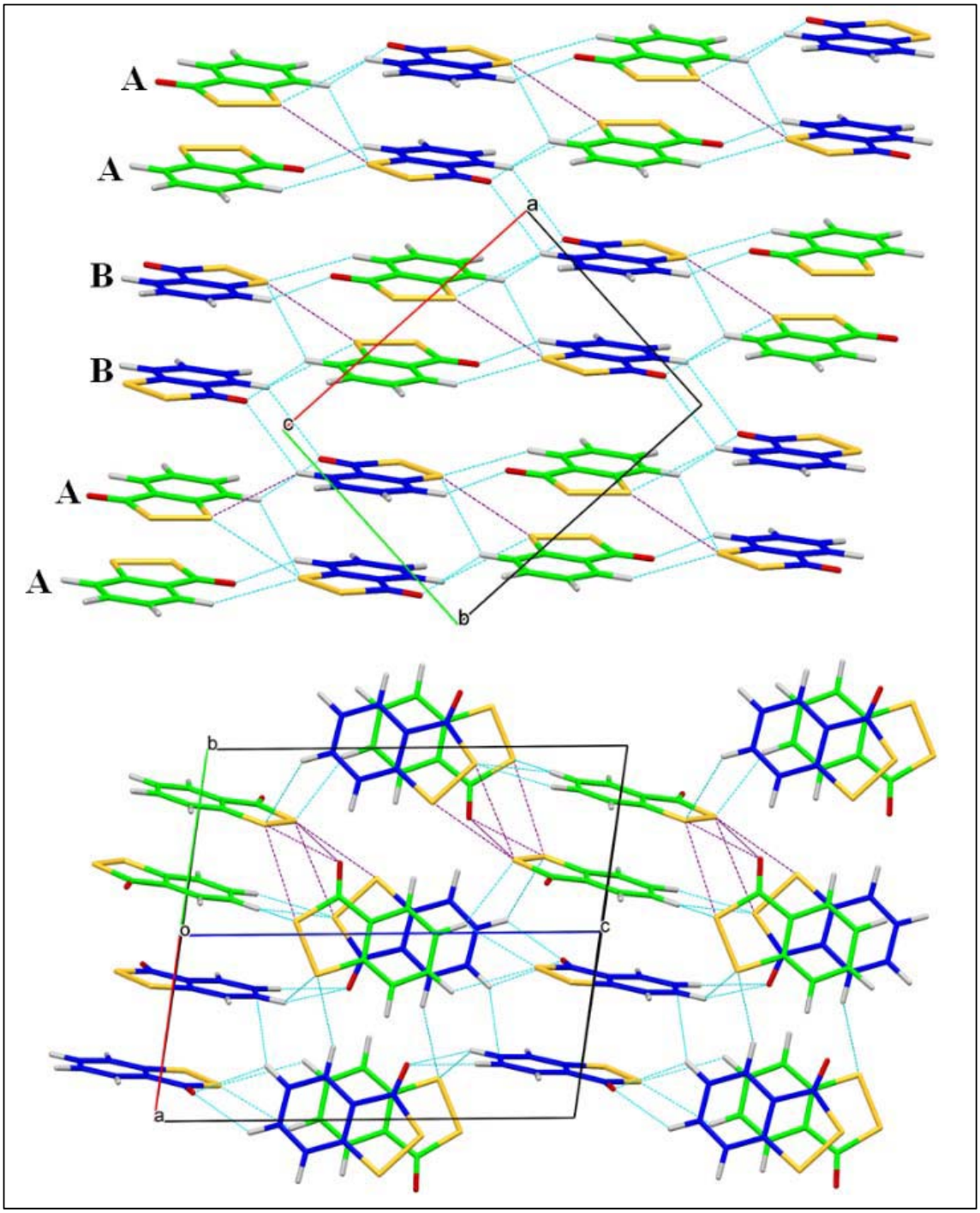

Figure S1. Crystal Packing of **COSS** Showing the Presence of π-Stacking, Hydrogen Bonding (cyan) and Chalcogen Bonding (purple) interactions.

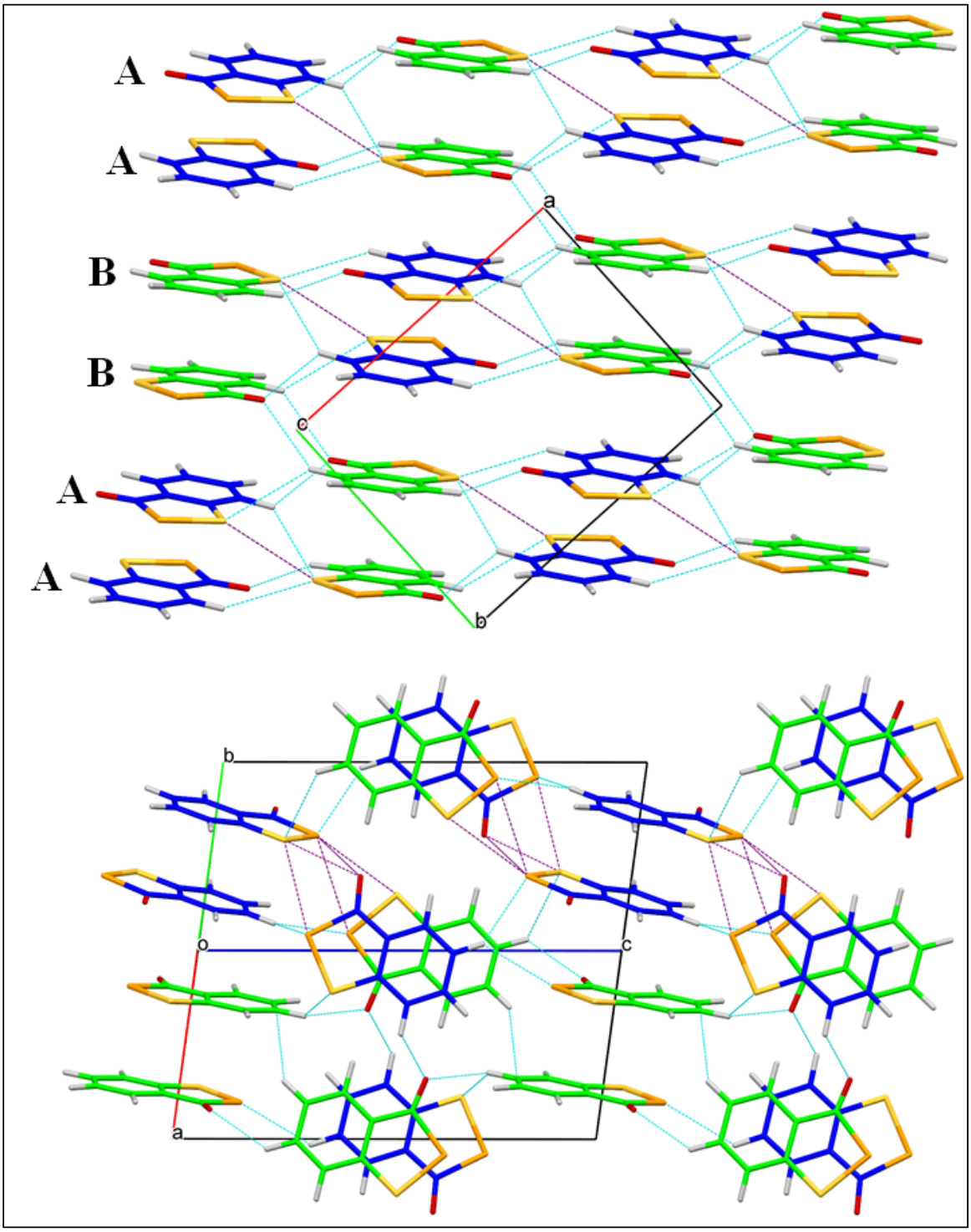

Figure S2. Crystal packing showing the presence of π-stacking, hydrogen bonding (in cyan) and chalcogen bonding (in purple) in **COSeS**.

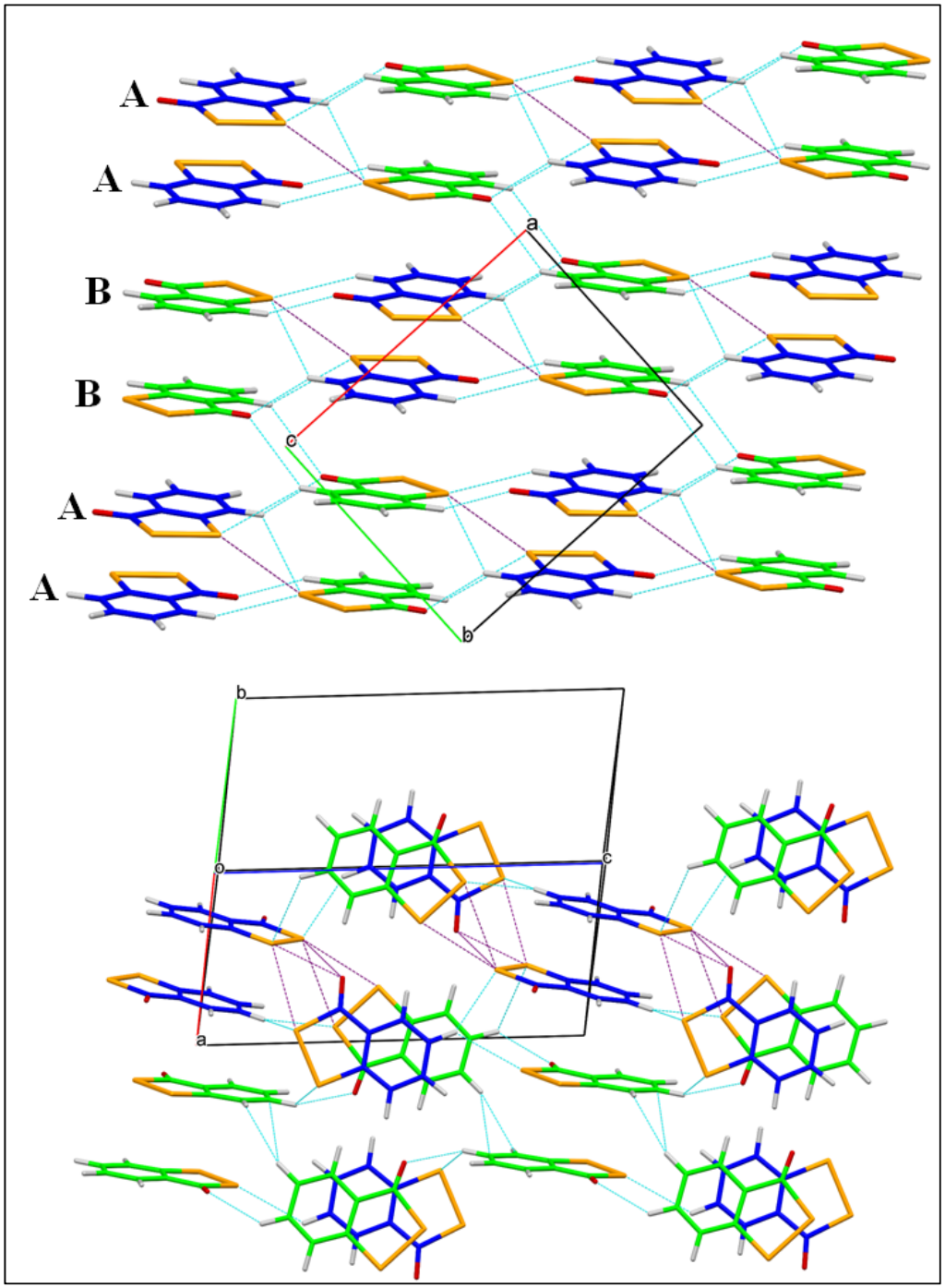

Figure S3. Crystal packing showing the presence of π-stacking, hydrogen bonding and chalcogen bonding in **COSeSe**.

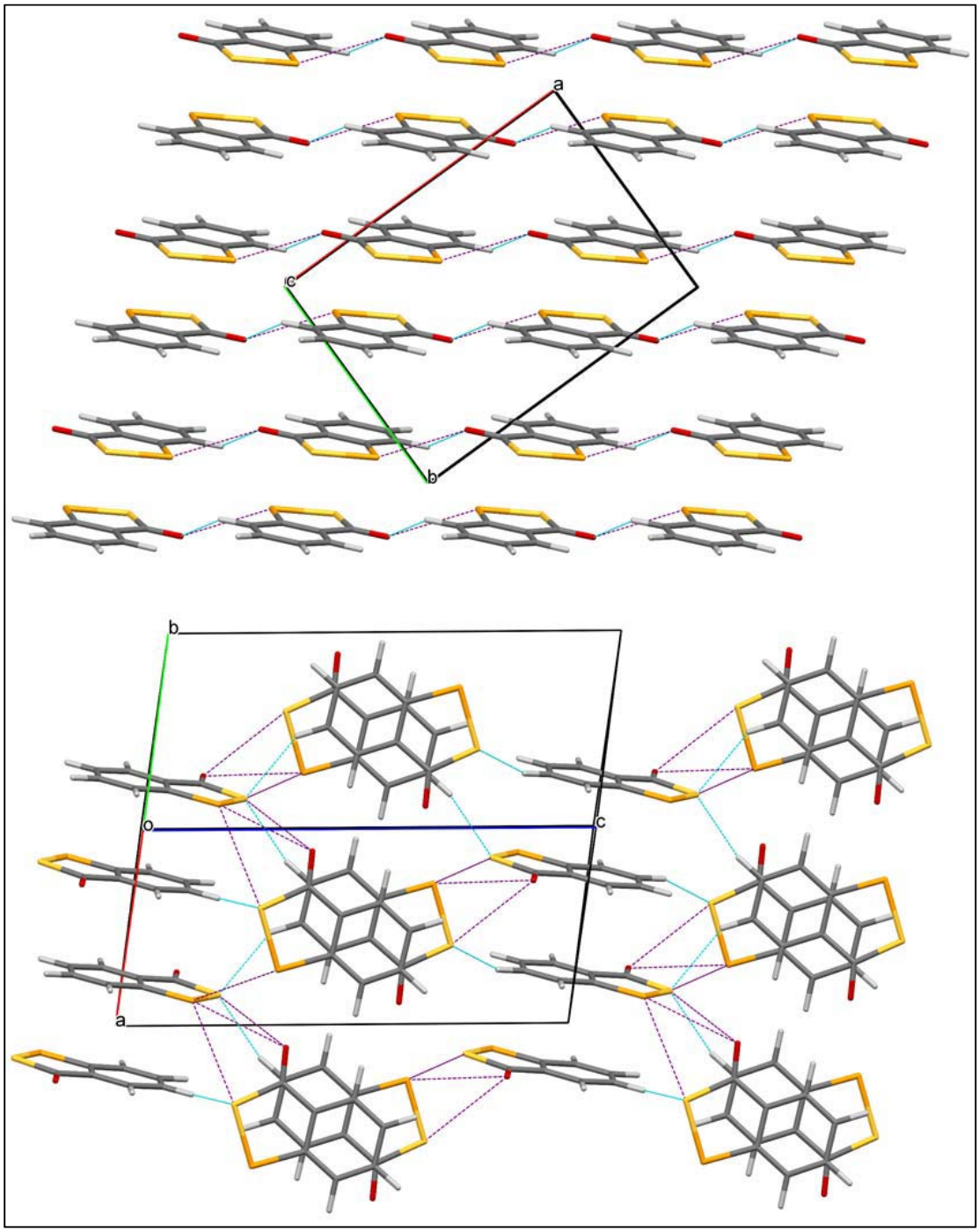

Figure S4 .Crystal packing showing the presence of π-stacking, hydrogen bonding (in cyan) and chalcogen bonding in **COSSe**.

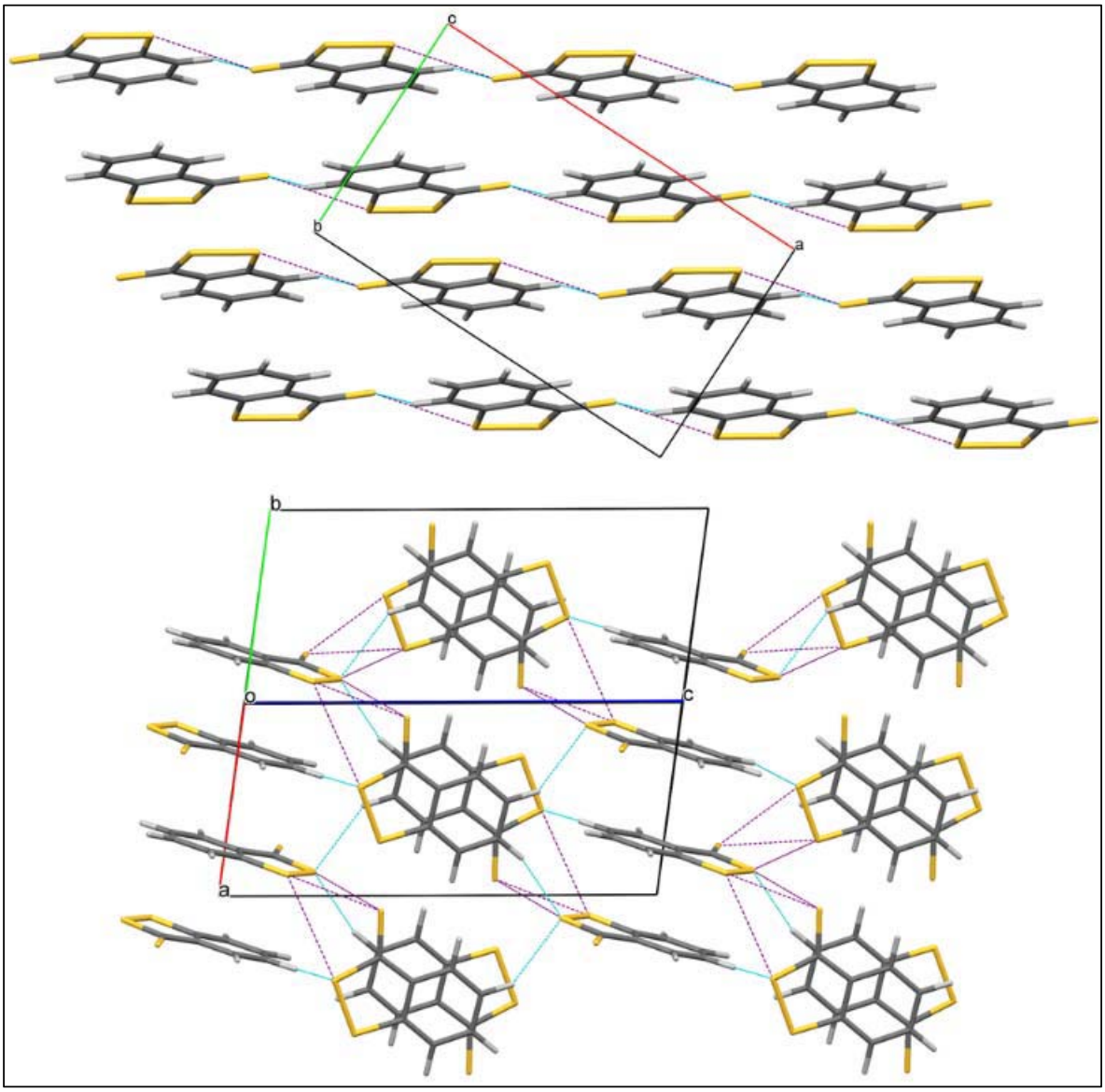

Figure S5. Crystal packing showing the presence of π-stacking, hydrogen bonding (cyan) and chalcogen bonding (purple) in **CSSS** (AYOZAR).

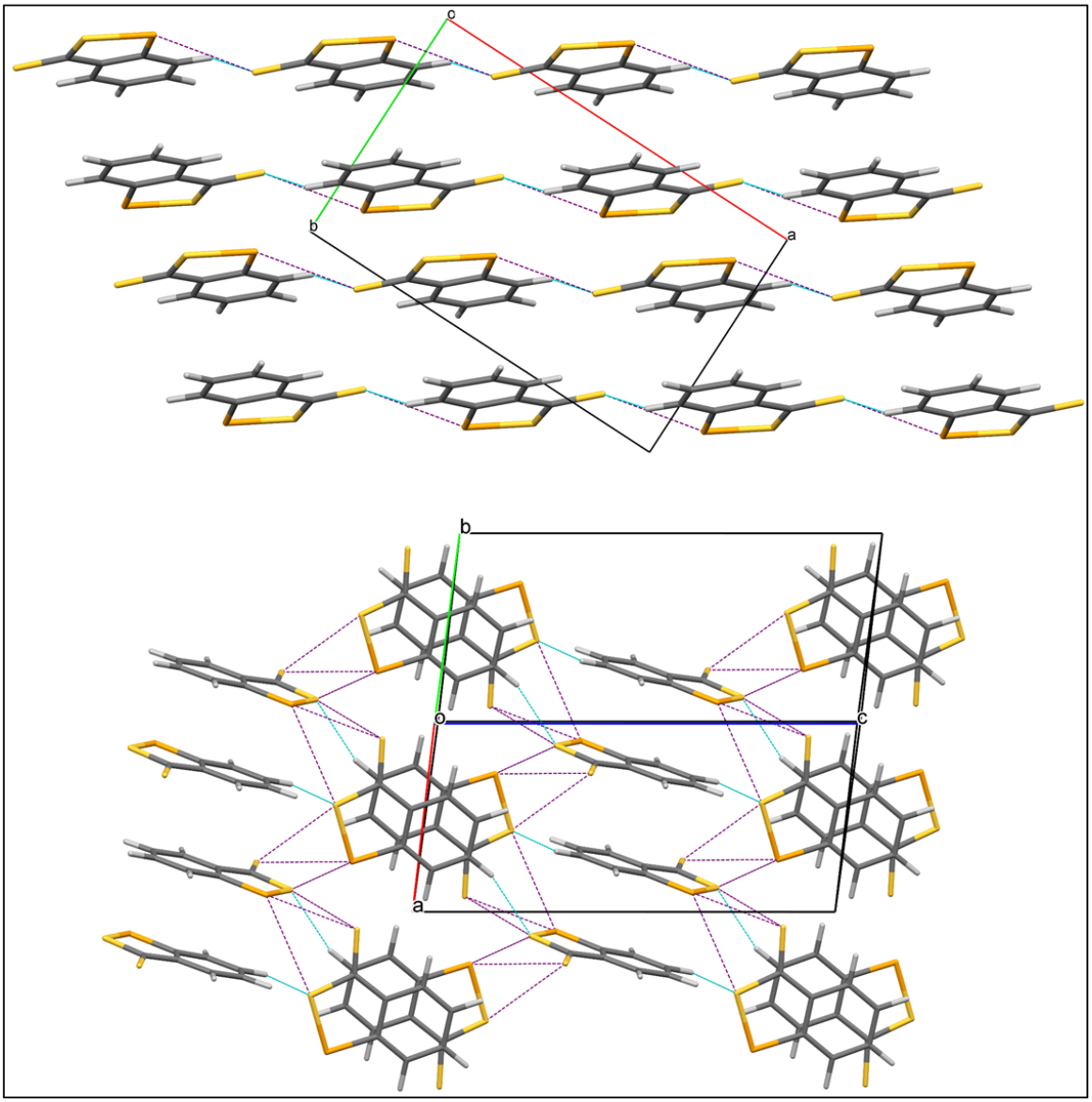

Figure S6. Crystal packing showing the presence of π-stacking, hydrogen bonding (in cyan) and chalcogen bonding (in purple) in **CSSSe**.

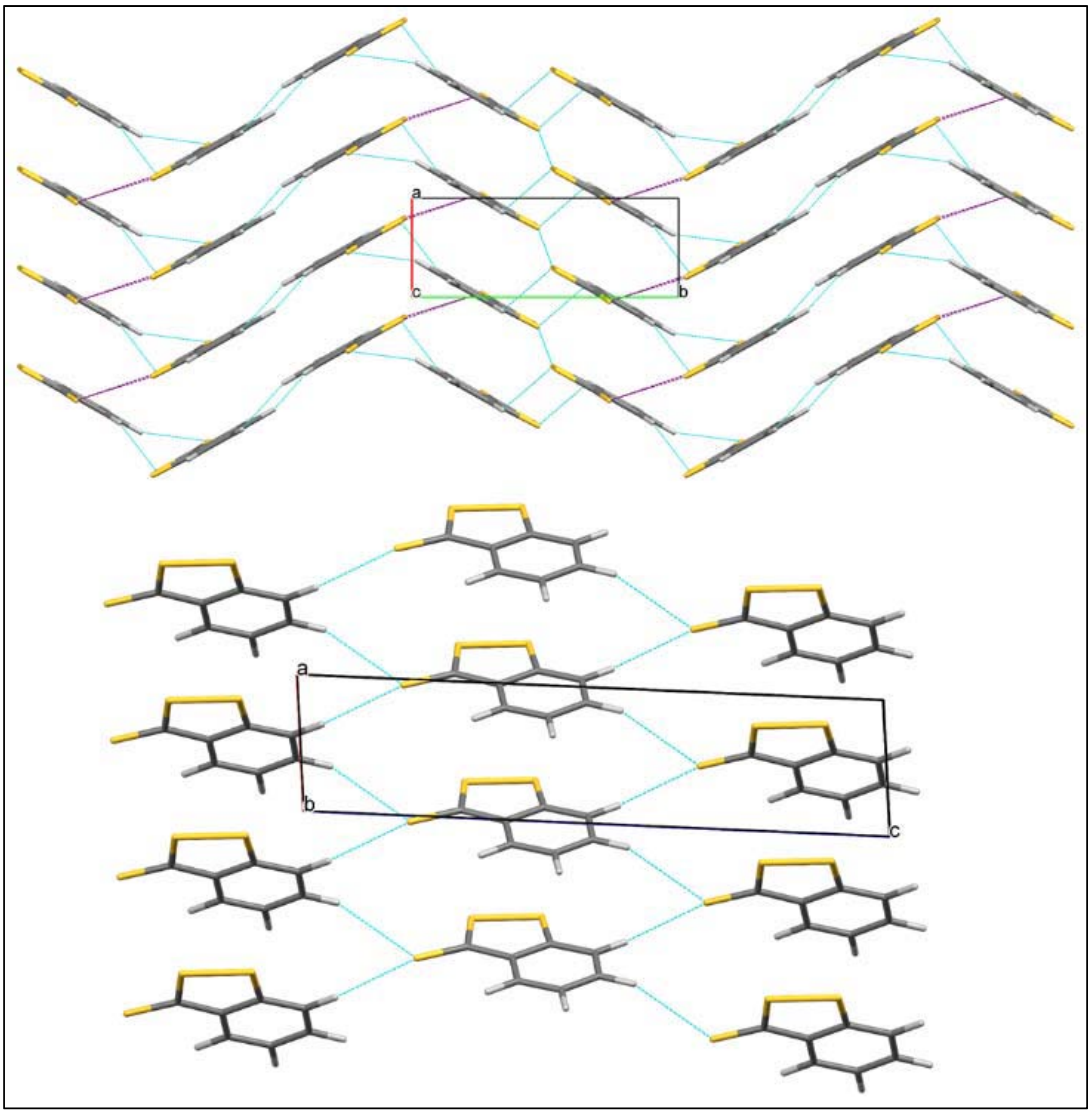

Figure S7. Crystal packing showing the presence of π-stacking, hydrogen bonding (in cyan) and chalcogen bonding (in purple) in **CSSS** (AYOZAR01).

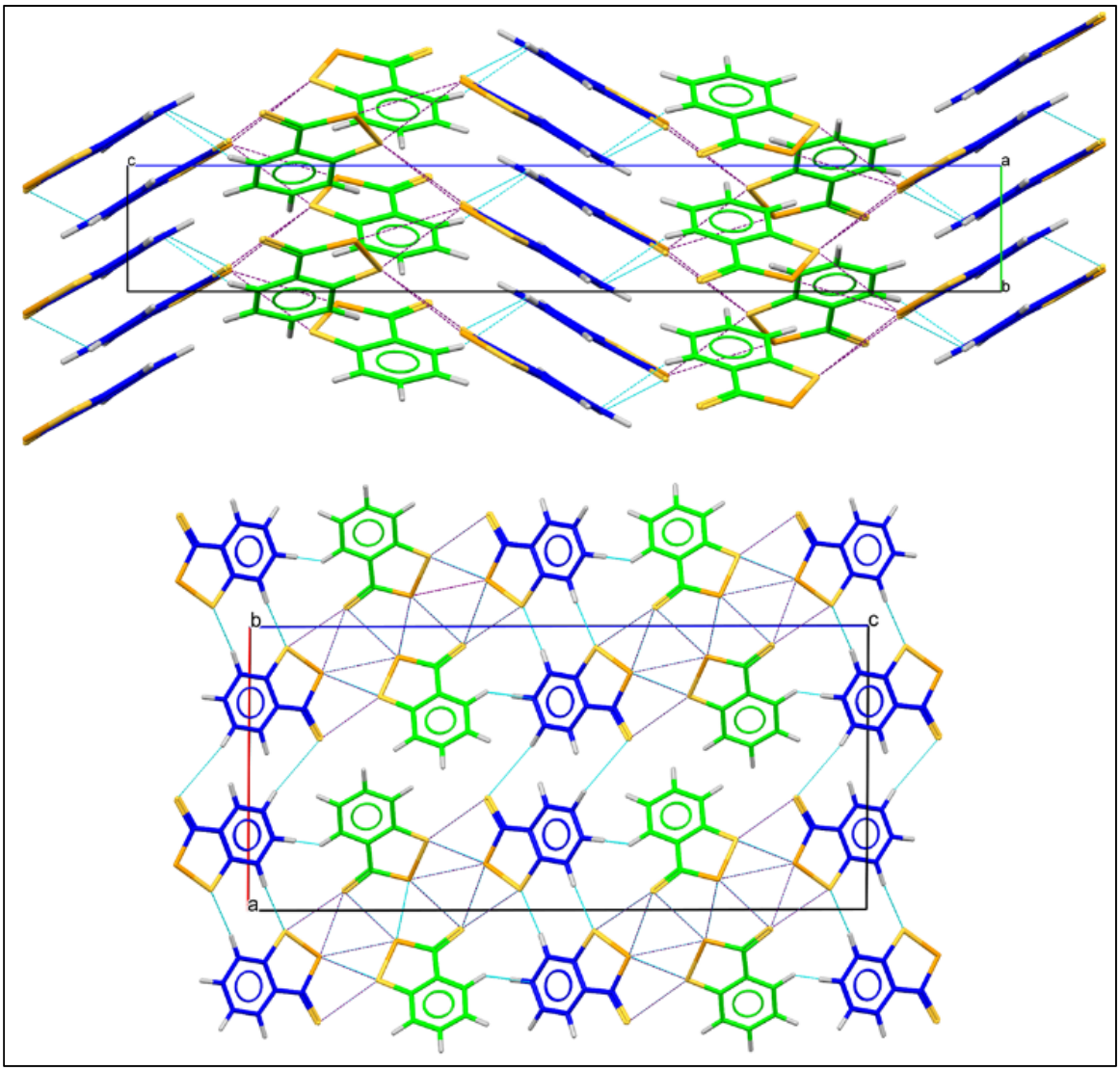

Figure S8. Crystal packing showing the presence of π-stacking, hydrogen bonding (in cyan) and chalcogen bonding (in purple) in **CSSeS**

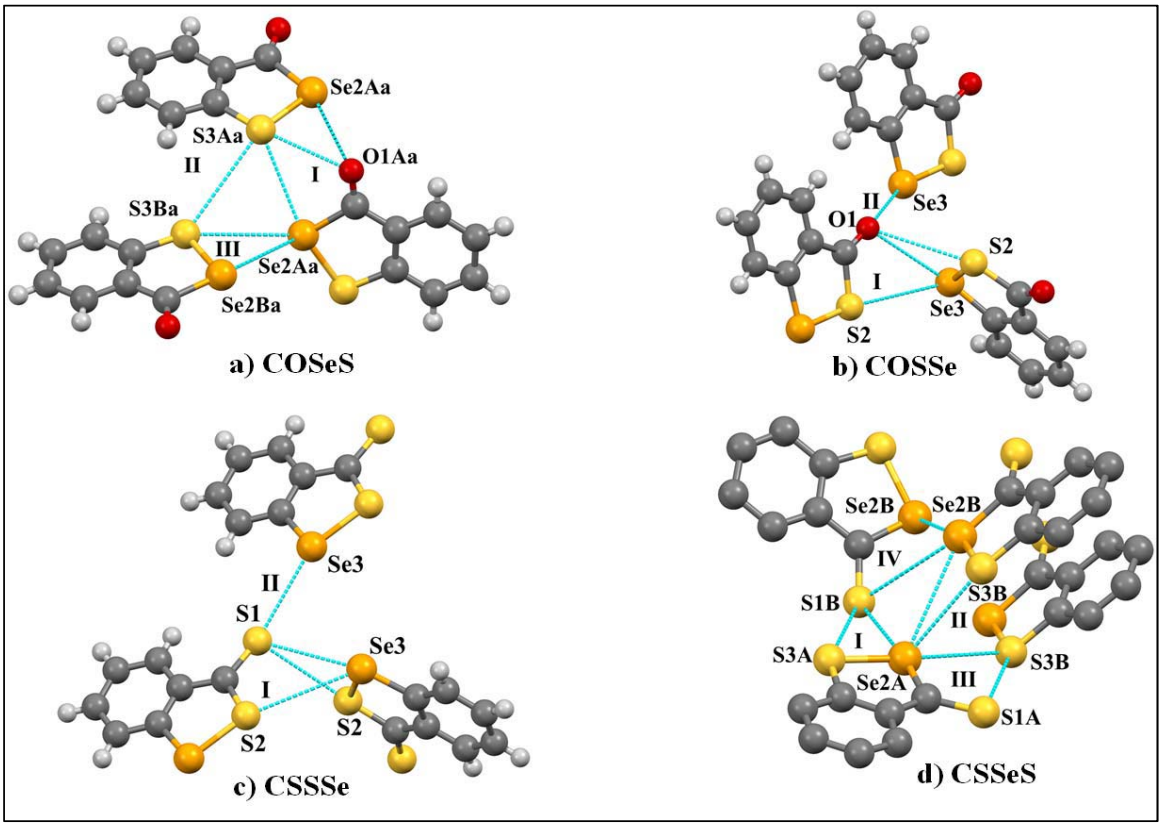

Figure S9. ChB motifs in (a) **COSeS,** (b) **COSSe,** (c) **CSSSe** and (d) **CSSeS.** Letters **A** and **B** in the atomic labels of **COSeS** and **CSSeS** report for two molecules present in the asymmetric unit. The letter **a** in the atomic labels of **COSeS** reports for the major molecular component in the disordered crystal structure.

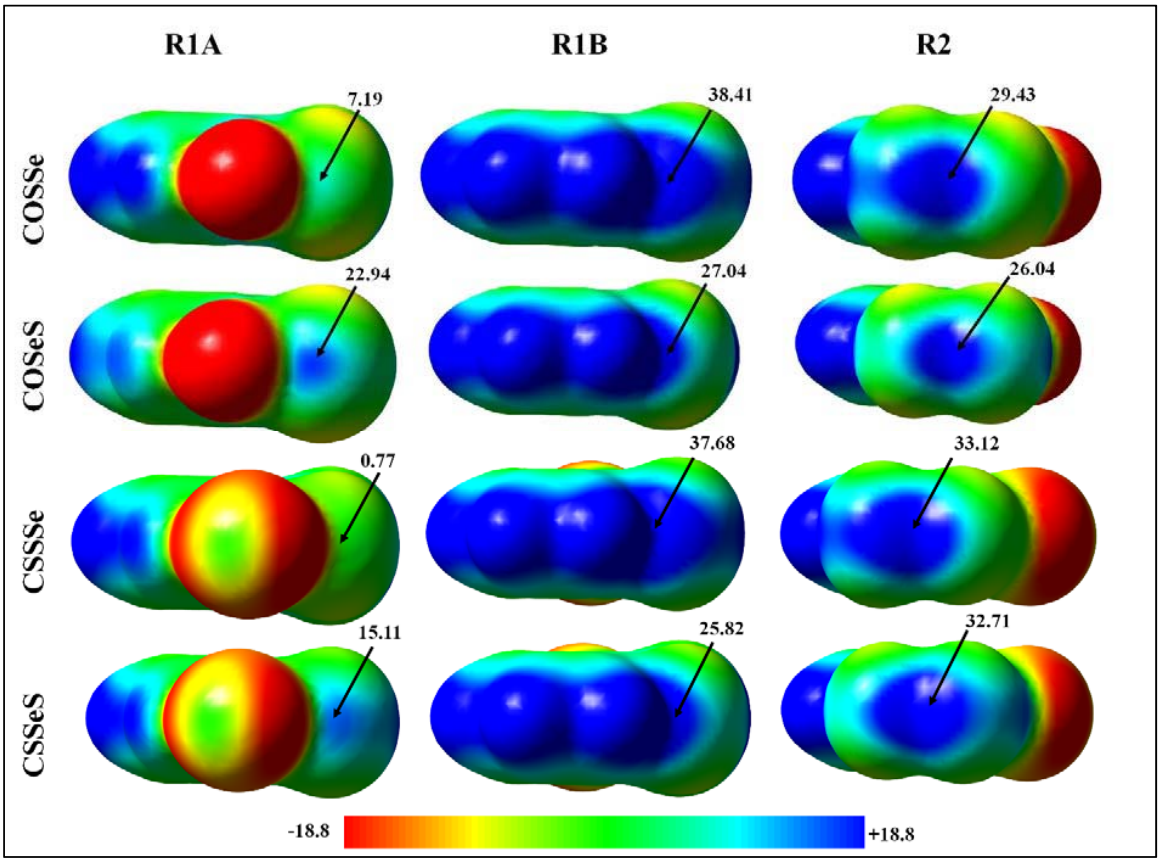

Figure S10. Electrostatic potential maps of **COSSe**, **COSeS**, **CSSSe** and **CSSeS** drawn along R1A, R1B and R2A regions. Maps are plotted on the iso-electron density surface $\rho = 0.002$ a.u. Blue: positive, Red: negative. The ESP values in the figure are reported in kcal/mol.

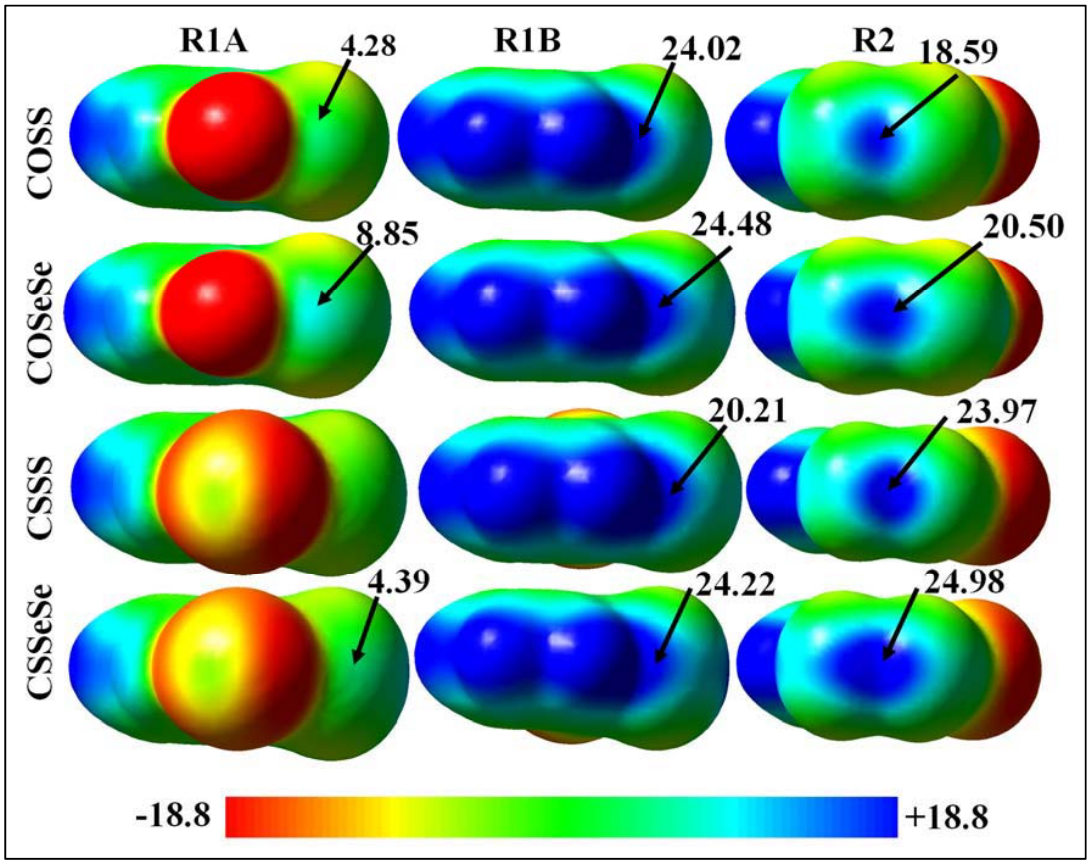

Figure S11. Electrostatic potential maps of **COSS**, **COSeSe**, **CSSS** and **CSSeSe** drawn along R1A, R1B and R2A regions. Maps are plotted on the iso-electron density surface $\rho = 0.001$ a.u. Blue: positive, Red: negative. The ESP values in the figure are reported in kcal/mol.

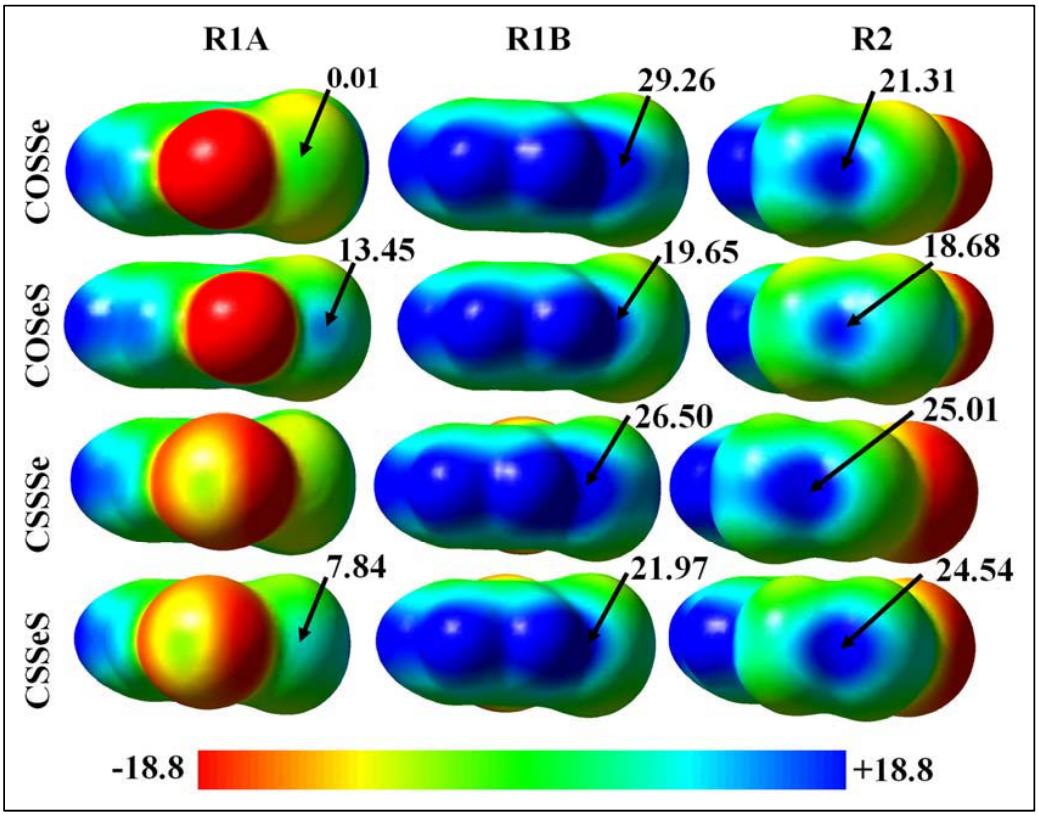

Figure S12. Electrostatic potential maps of **COSSe**, **COSeS**, **CSSSe** and **CSSeS** drawn along R1A, R1B and R2A regions. Maps are plotted on the iso-electron density surface $\rho = 0.001$ a.u. Blue: positive, Red: negative. The ESP values in the figure are reported in kcal/mol.

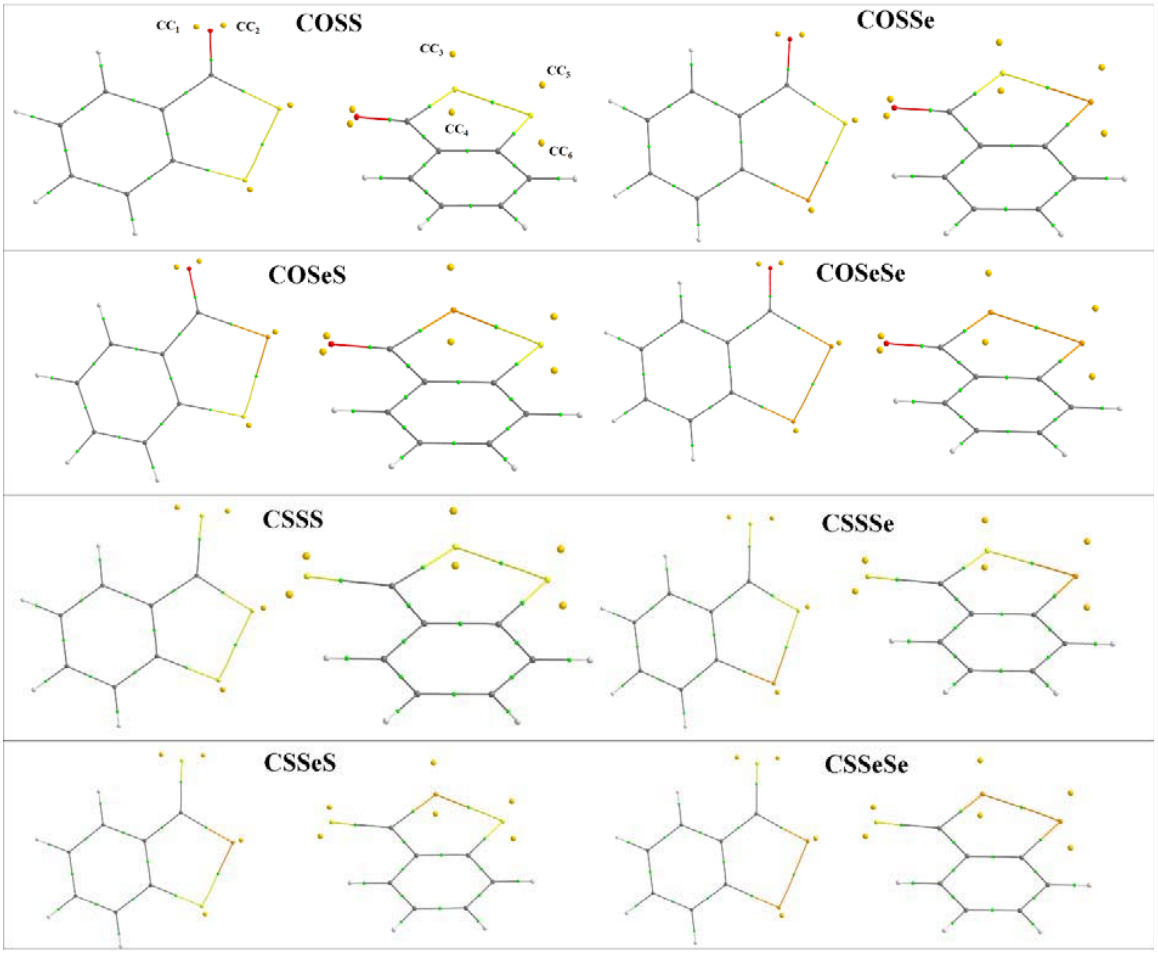

Figure S13. (3,-3) CPs of L(**r**) (in yellow) representing the lone-pairs of the chalcogen atoms present in the molecule.

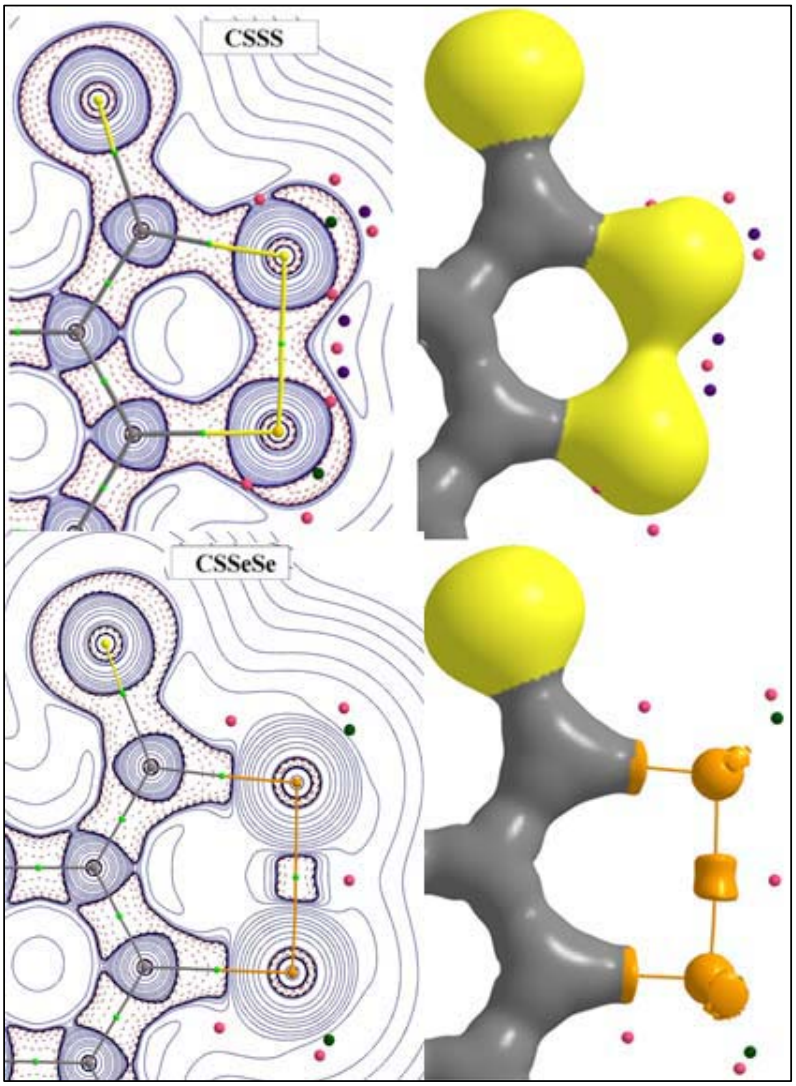

Figure S14. Left: $L(\mathbf{r}) = -\nabla^2\rho(\mathbf{r})$ maps [contours in e/Å^5 are in logarithmic scale: positive (red) and negative (blue)] for **CSSS** (top) and **CSSeSe** (bottom). Right: $\nabla^2\rho(\mathbf{r}) = 0$ maps plotted for **CSSS** (top) and **CSSeSe** (bottom) with atomic portioning. Relevant CPs of $L(\boldsymbol{r})$ in the valence shell of chalcogen atoms are denoted in maps as small spheres [(3, −1) CPs are green, (3, +1) CPs are pink and (3, +3) CPs are violet]. (3,-3) CPs corresponding to *lone-pairs* of Ch2 and Ch3 are out of plane in the left and hidden by the enclosing surfaces $\nabla^2\rho(\mathbf{r}) = 0$ in the right. They are shown in Figure S13.

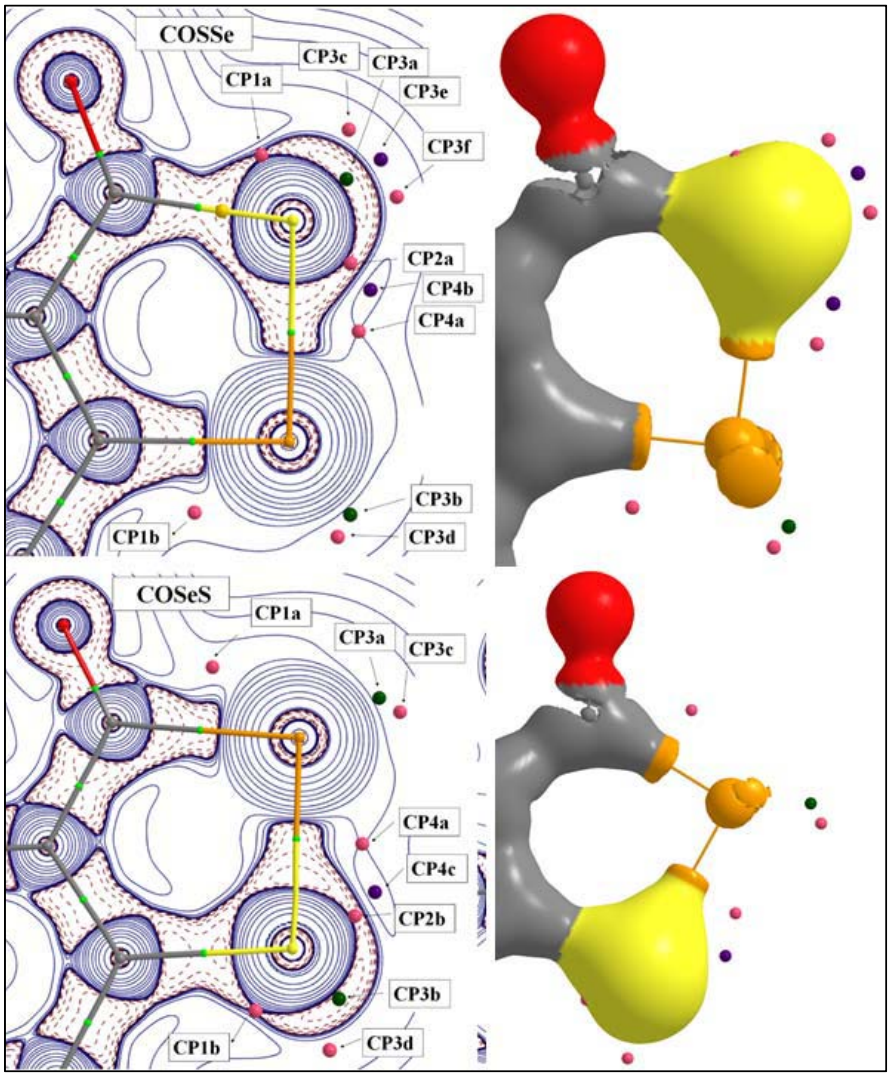

Figure S15. Left: $L(\mathbf{r}) = -\nabla^2\rho(\mathbf{r})$ maps [contours in e/Å^5 are in logarithmic scale: positive (red) and negative (blue)] for **COSSe** (top) and **COSeS** (bottom). Right: $\nabla^2\rho(\mathbf{r}) = 0$ maps plotted for **COSSe** (top) and **COSeS** (bottom) with atomic portioning. Relevant CPs of $L(\boldsymbol{r})$ in the valence shell of chalcogen atoms are denoted in maps as small spheres [(3, −1) CPs are green, (3, +1) CPs are pink and (3, +3) CPs are violet]. (3,-3) CPs corresponding to *lone-pairs* of Ch2 and Ch3 are out of plane in the left and hidden by the enclosing surfaces $\nabla^2\rho(\mathbf{r}) = 0$ in the right. They are shown in Figure S13.

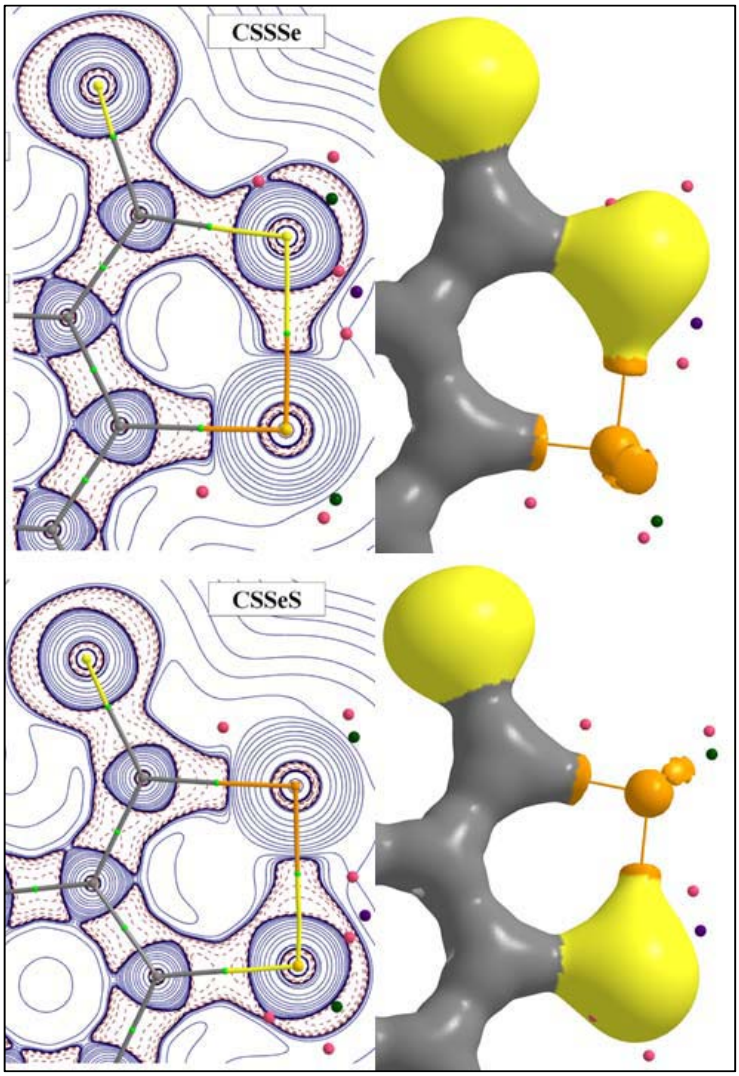

Figure S16. Left: $L(\mathbf{r}) = -\nabla^2\rho(\mathbf{r})$ maps [e/Å^5 , contours are in logarithmic scale: positive (red) and negative (blue)] for **CSSSe** (top) and **CSSeS** (bottom). Right: $\nabla^2\rho(\mathbf{r}) = 0$ maps plotted for **CSSSe** (top) and **CSSeS** (bottom) with atomic portioning. Relevant CPs of $L(\boldsymbol{r})$ in the valence shell of chalcogen atoms are denoted in maps as small spheres [(3, −1) CPs are green, (3, +1) CPs are pink and (3, +3) CPs are violet]. (3,-3) CPs corresponding to *lone-pairs* of Ch2 and Ch3 are out of plane in the left and hidden by the enclosing surfaces $\nabla^2\rho(\mathbf{r}) = 0$ in the right. They are shown in Figure S13.

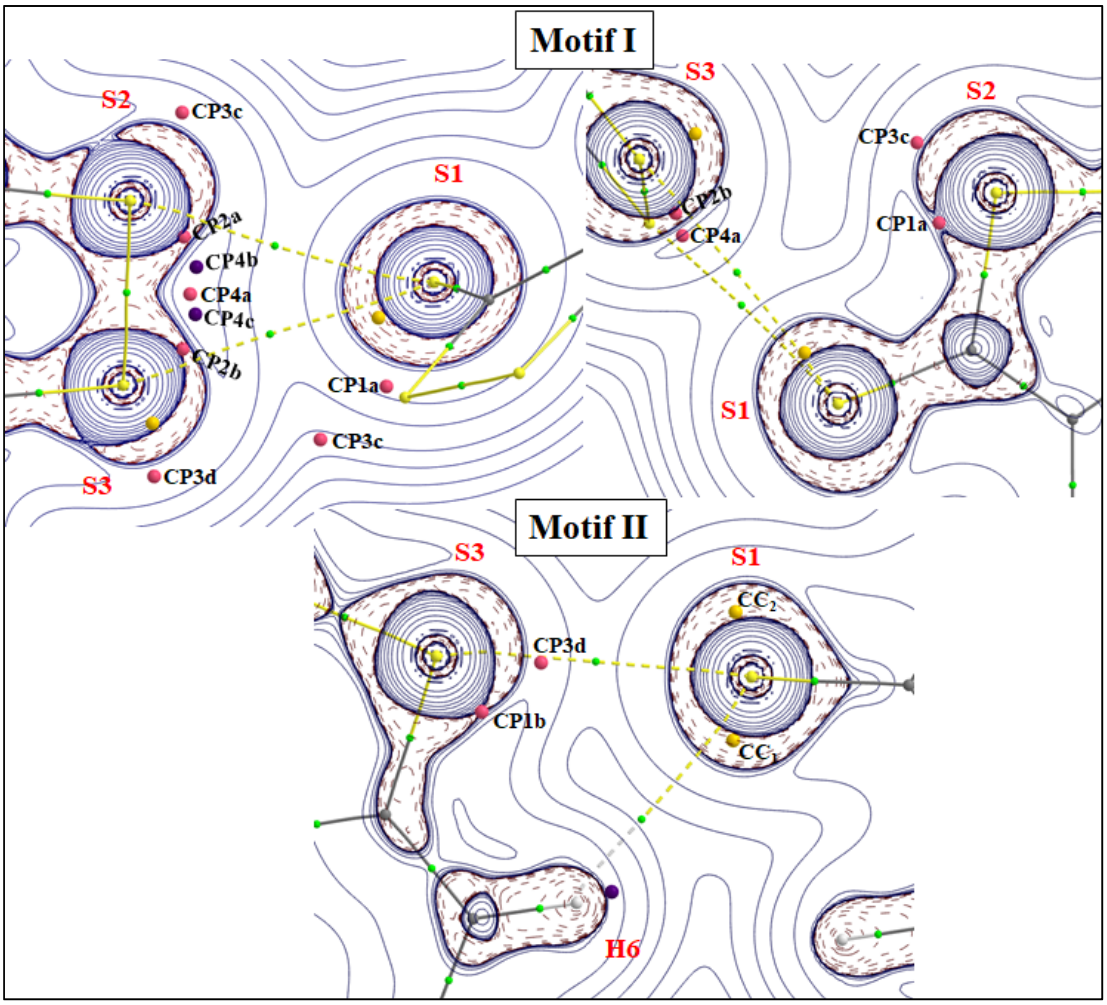

Figure S17 Intermolecular bond critical points (BCPs, small green spheres), intermolecular bond paths (dashed lines) and relevant charge concentration and charge depletion (CC/CD) sites (yellow/pink/violet spheres) involved in the chalcogen bonding interactions present in motifs **I** and **II** of **CSSS** (AYOZAR). The CPs of $L(\mathbf{r})$ are: (3,−3) in yellow, (3+1) in pink, and (3,+3) in violet.

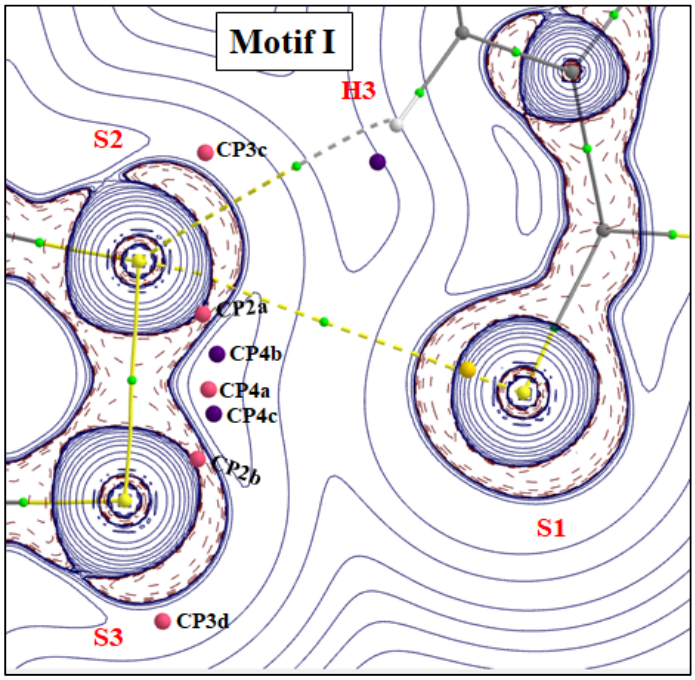

Figure S18 Intermolecular bond critical points (BCPs, small green spheres), intermolecular bond paths (dashed lines) and relevant charge concentration and charge depletion (CC/CD) sites (yellow/pink/violet spheres) involved in the chalcogen bonding interactions present in motif **I** of **CSSS** (AYOZAR01). The CPs of $L(\mathbf{r})$ are: (3,−3) in yellow, (3+1) in pink, and (3,+3) in violet.

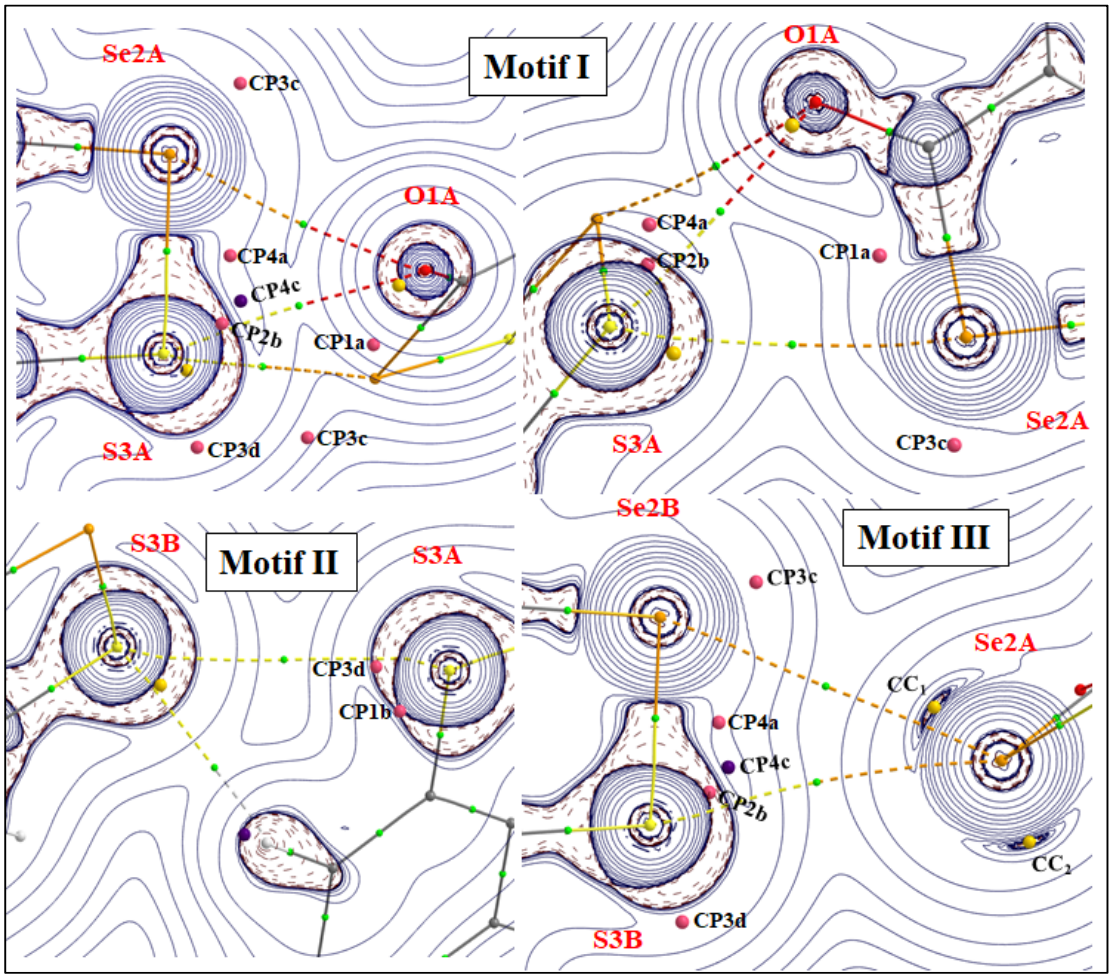

Figure S19 Intermolecular bond critical points (BCPs, small green spheres), intermolecular bond paths (dashed lines) and relevant charge concentration and charge depletion (CC/CD) sites (yellow/pink/violet spheres) involved in the chalcogen bonding interactions present in motifs **I**, **II** and **III** of **COSeS**. The CPs of $L(\mathbf{r})$ are: (3,−3) in yellow, (3+1) in pink, and (3,+3) in violet.

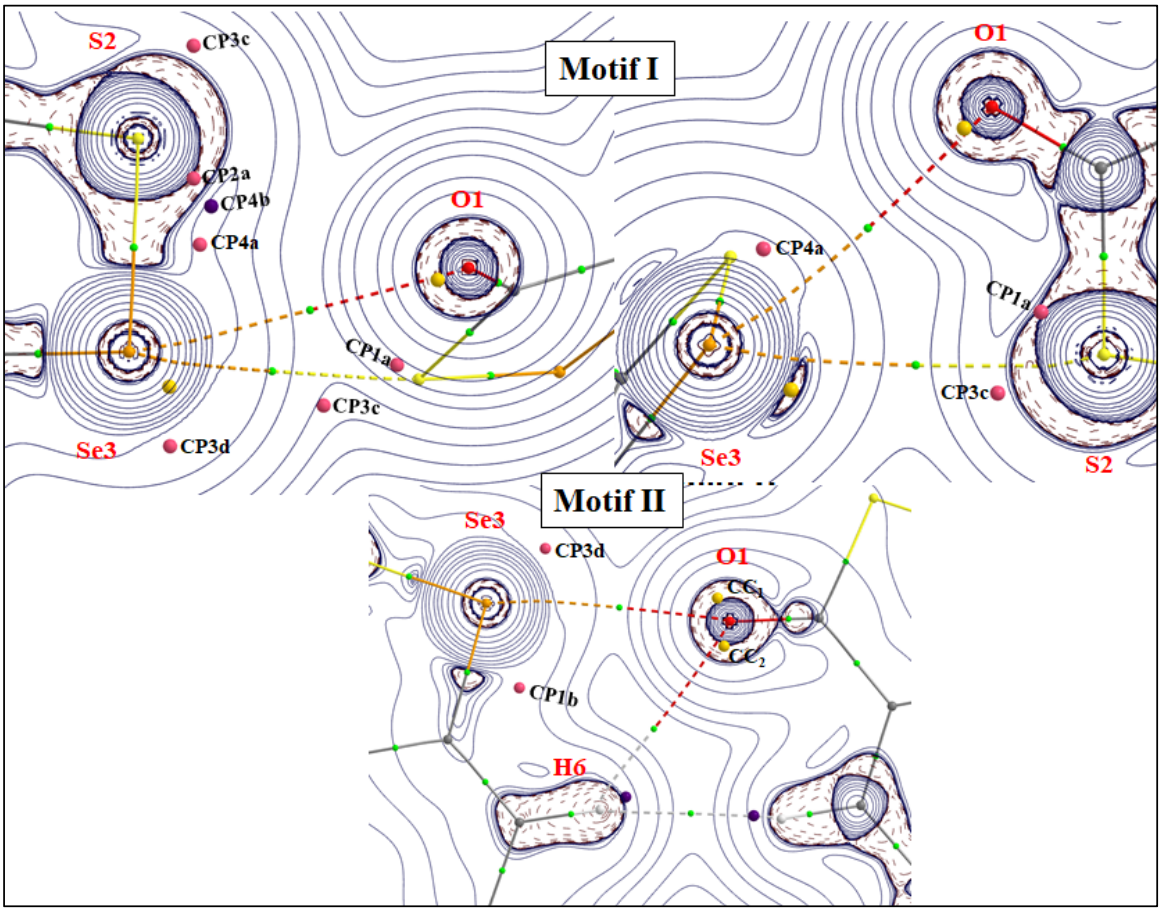

Figure S20 Intermolecular bond critical points (BCPs, small green spheres), intermolecular bond paths (dashed lines) and relevant charge concentration and charge depletion (CC/CD) sites (yellow/pink/violet spheres) involved in the chalcogen bonding interactions present in motifs **I** and **II** of **COSSe**. The CPs of $L(\mathbf{r})$ are: (3,−3) in yellow, (3+1) in pink, and (3,+3) in violet.

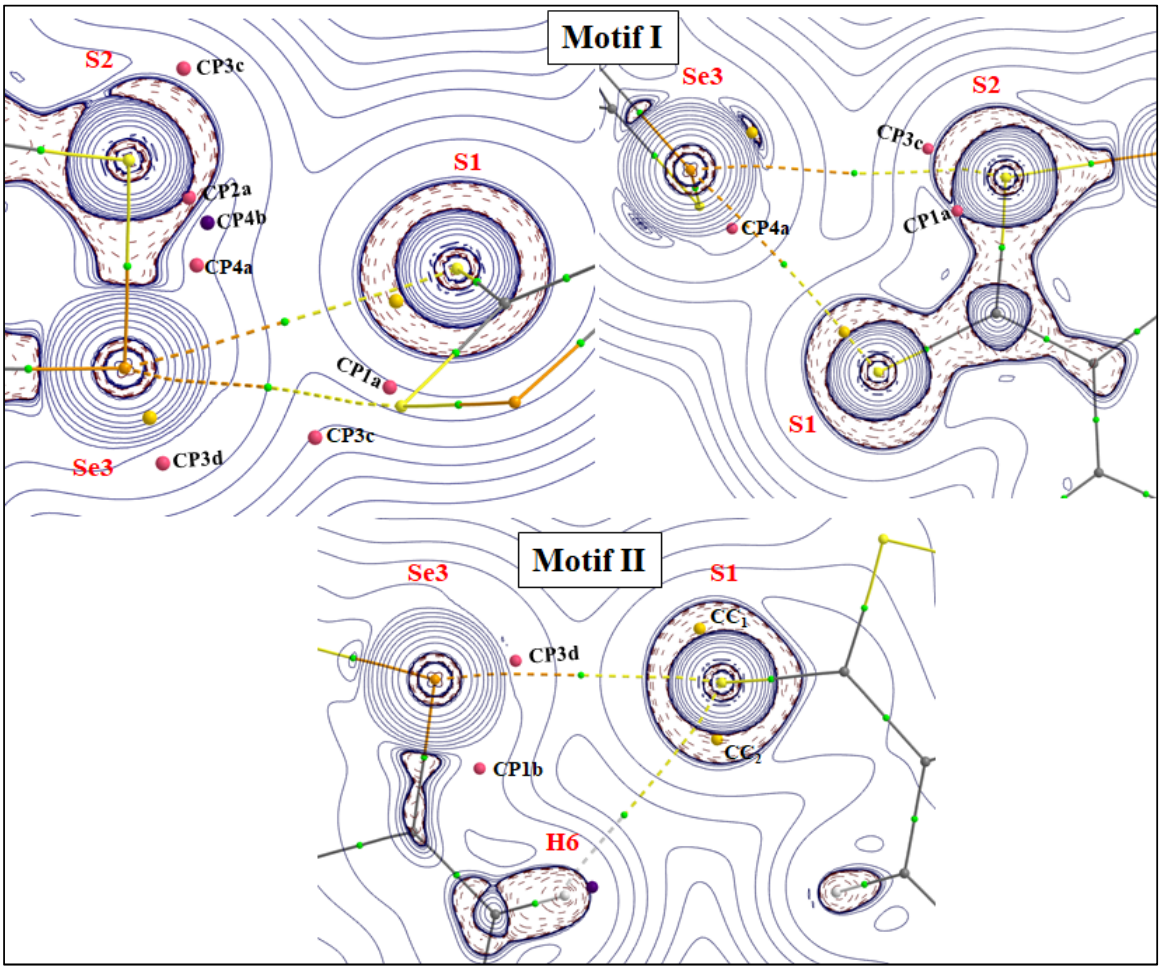

Figure S21 Intermolecular bond critical points (BCPs, small green spheres), intermolecular bond paths (dashed lines) and relevant charge concentration and charge depletion (CC/CD) sites (yellow/pink/violet spheres) involved in the chalcogen bonding interactions present in motifs **I** and **II** of **CSSSe** (AYOZAR). The CPs of $L(\mathbf{r})$ are: (3,−3) in yellow, (3+1) in pink, and (3,+3) in violet.

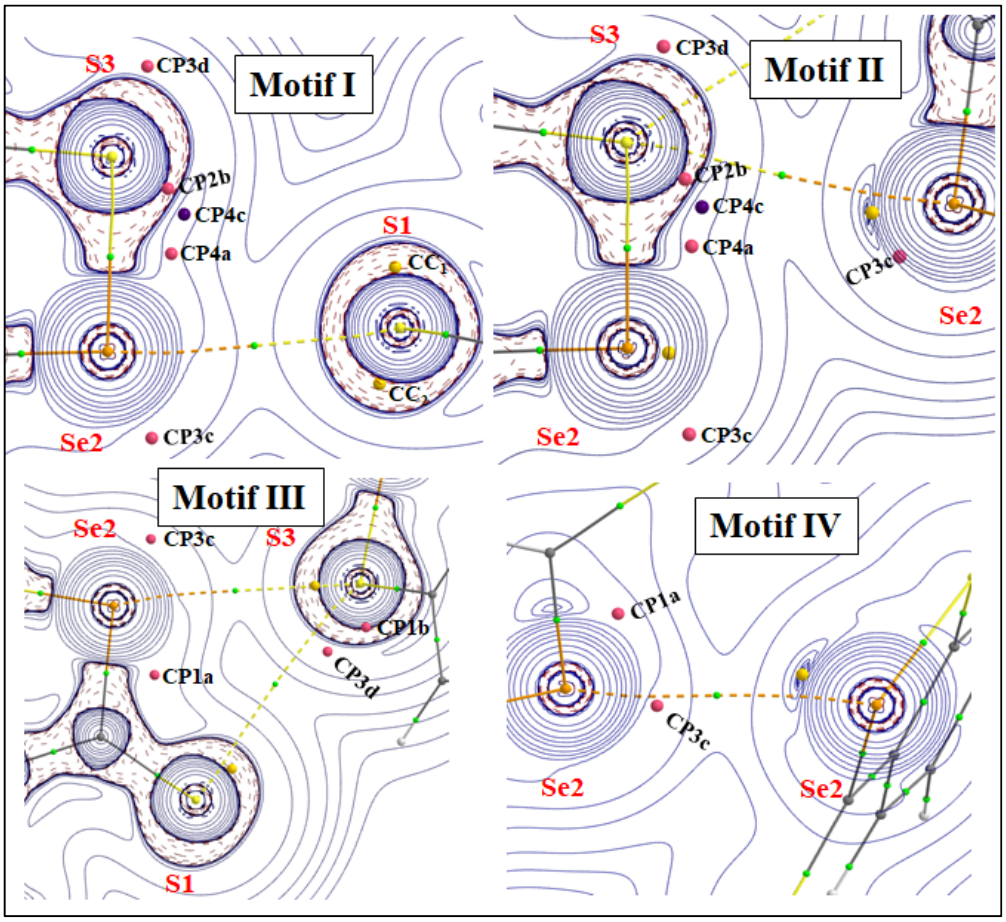

Figure S22 Intermolecular bond critical points (BCPs, small green spheres), intermolecular bond paths (dashed lines) and relevant charge concentration and charge depletion (CC/CD) sites (yellow/pink/violet spheres) involved in the chalcogen bonding interactions present in motifs **I**, **II**, **III** and **IV** of **CSSeS** (AYOZAR). The CPs of $L(\mathbf{r})$ are: (3,−3) in yellow, (3+1) in pink, and (3,+3) in violet.

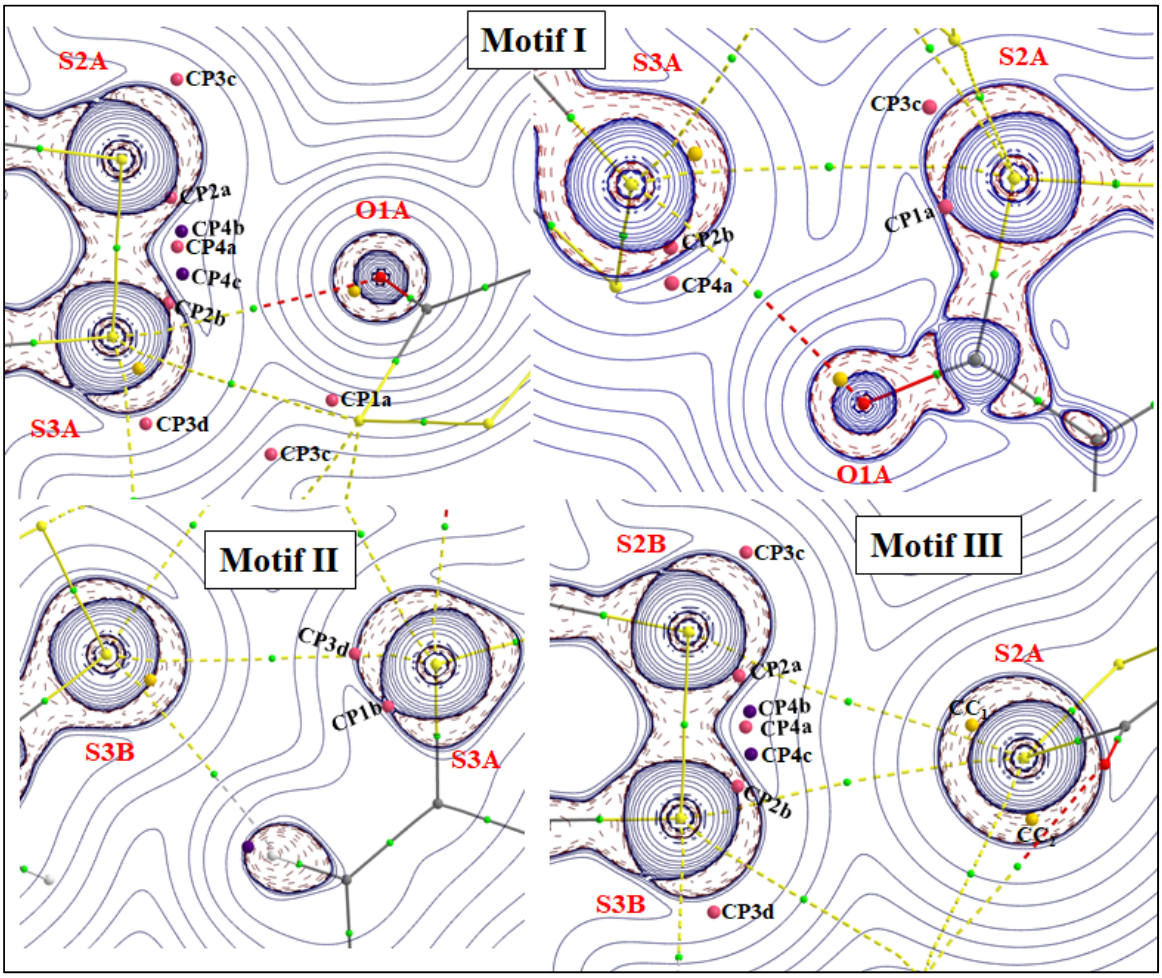

Figure S23 Intermolecular bond critical points (BCPs, small green spheres), intermolecular bond paths (dashed lines) and relevant charge concentration and charge depletion (CC/CD) sites (yellow/pink/violet spheres) involved in the chalcogen bonding interactions present in motifs **I**, **II** and **III** of **COSS** computed in trimer. The CPs of $L(\mathbf{r})$ are: (3,−3) in yellow, (3+1) in pink, and (3,+3) in violet.

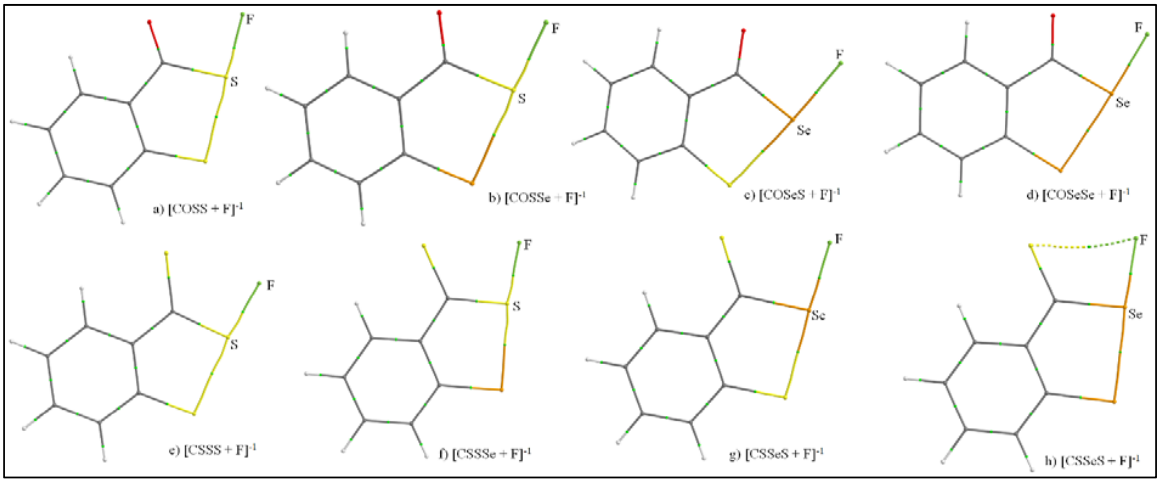

Figure S24. Molecular graphs for [**CCh1Ch2Ch3** + F]$^{-1}$ complexes formed via region R1A.

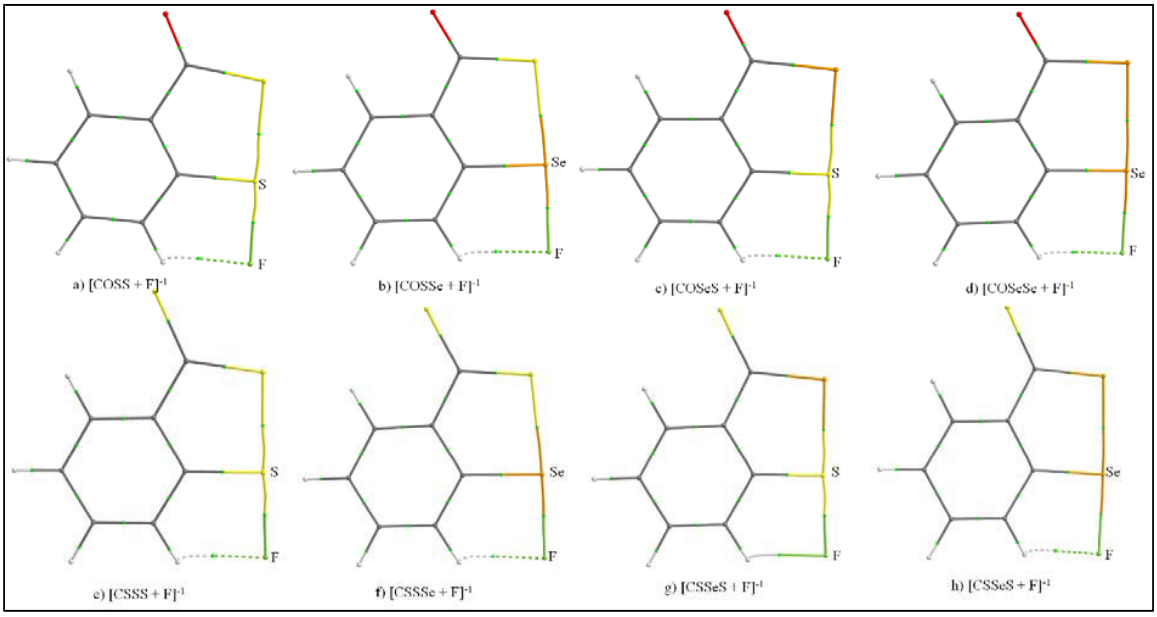

Figure S25. Molecular graphs for [**CCh1Ch2Ch3** + F]$^{-1}$ complexes formed via region R1B.

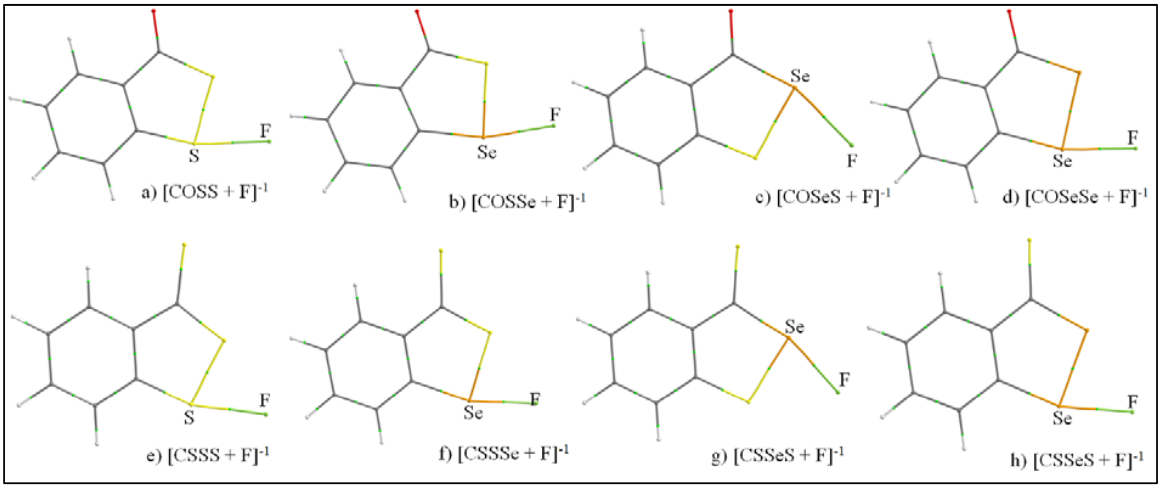

Figure S26. Molecular graphs for [**CCh1Ch2Ch3** + F]$^{-1}$ complexes formed via region R2.

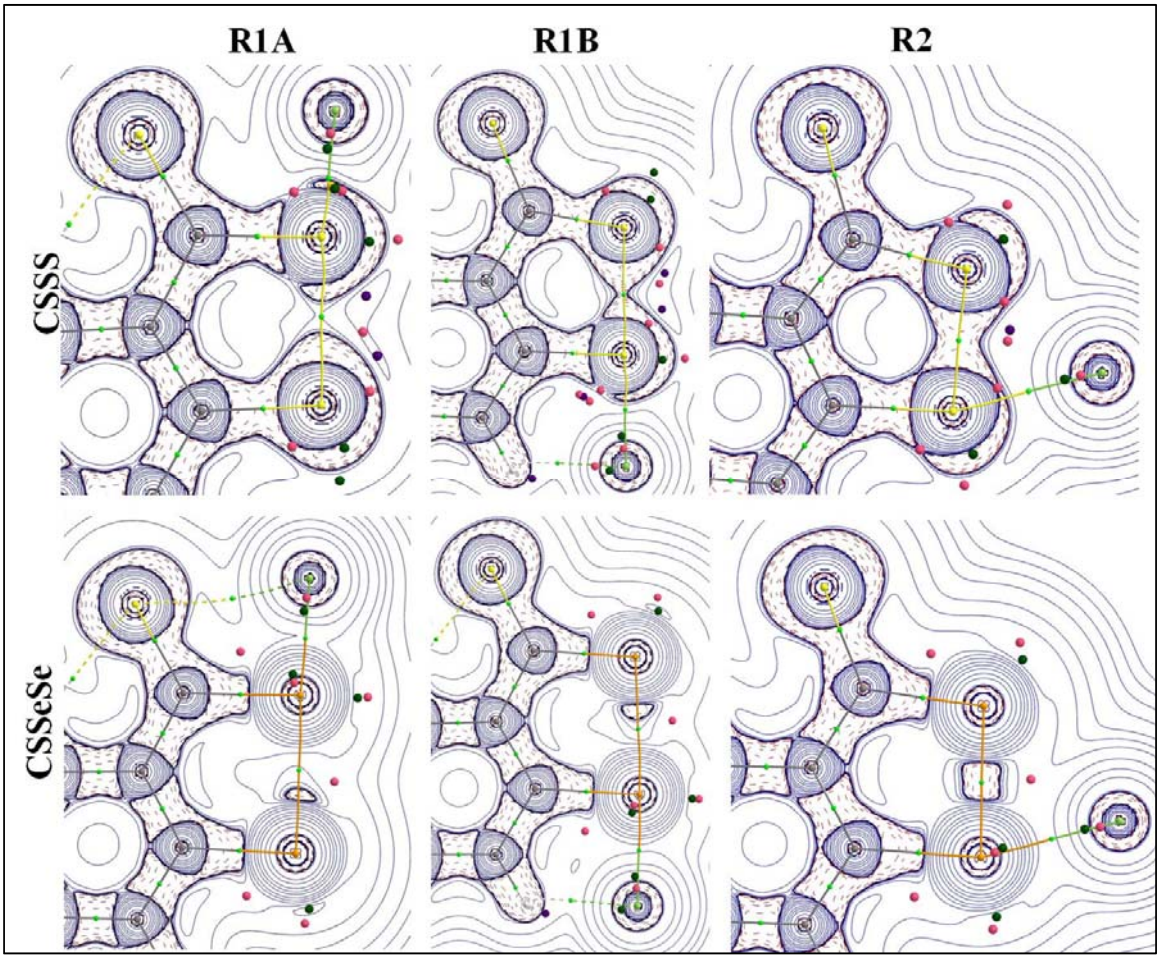

Figure S27 *L*(**r**) maps and CPs in fluoride adducts of **CSSS** (top) and **CSSeSe** (bottom). (3,+1) CPs (pink spheres) and (3,-1) CPs (dark green spheres) are depicted around Ch2, Ch3 and F atoms. Bond critical points are small light green spheres.

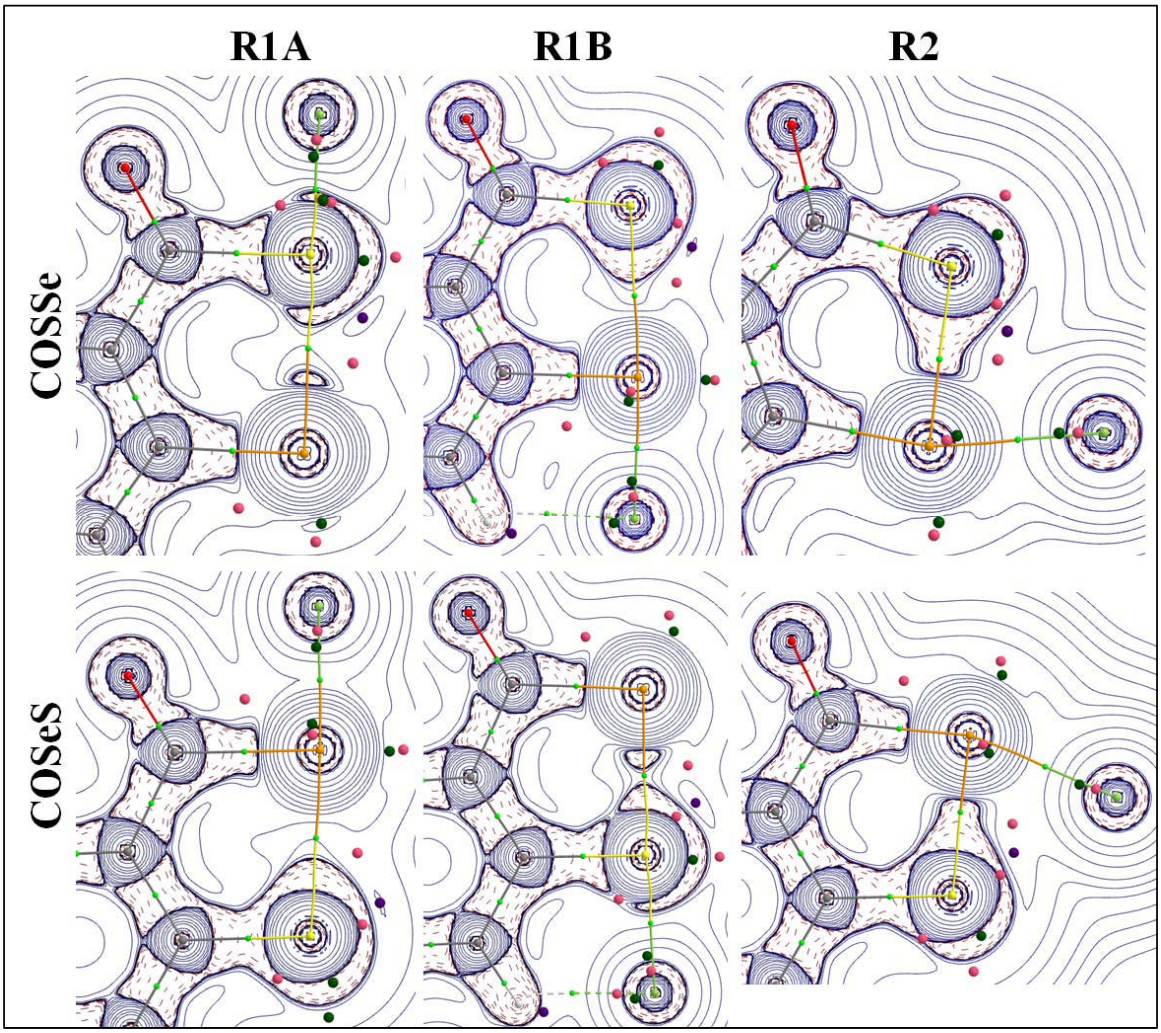

Figure S28 *L*(**r**) maps and CPs in fluoride adducts of **COSSe** (top) and **COSeS**(bottom). (3,+1) CPs (pink spheres) and (3,-1) CPs (dark green spheres) are depicted around Ch2, Ch3 and F atoms. Bond critical points are small light green spheres.

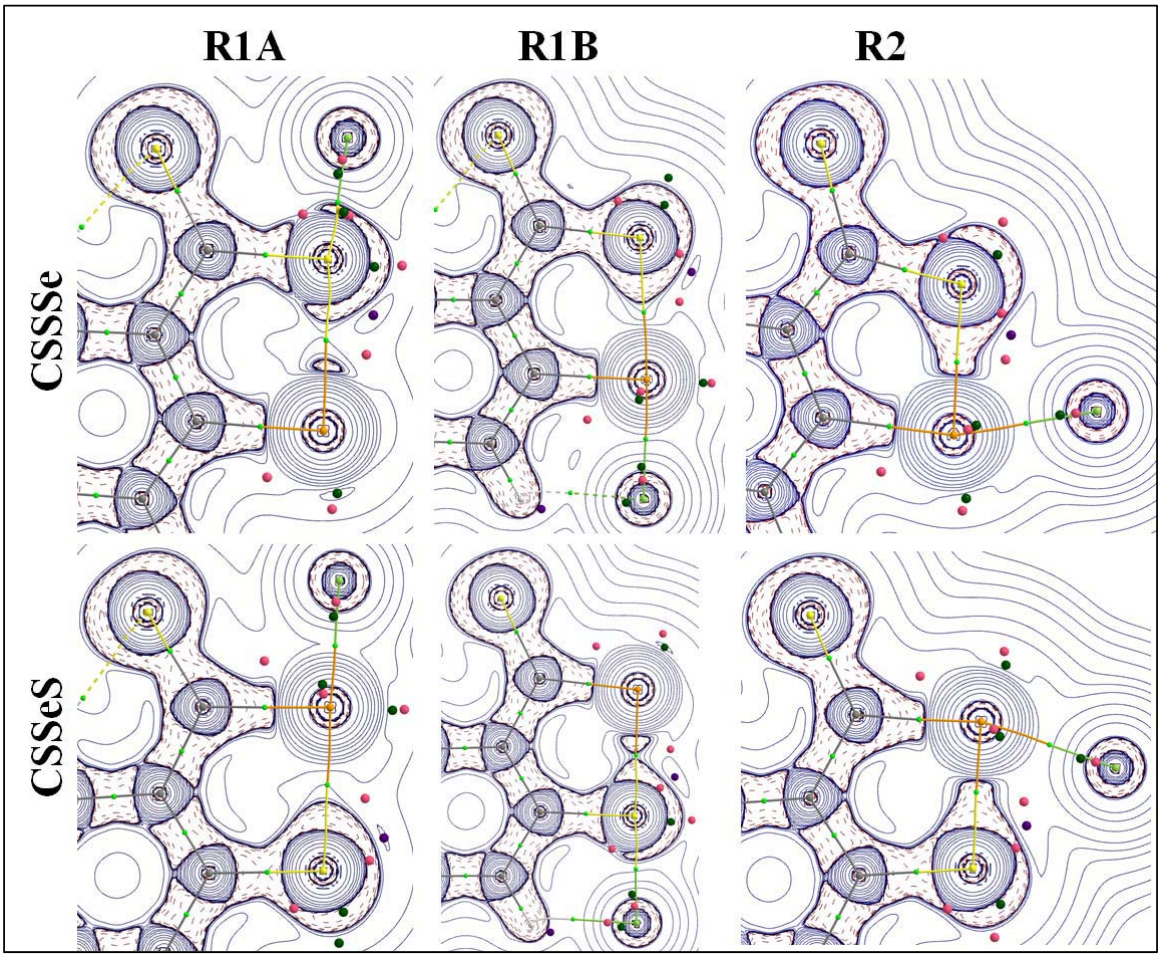

Figure S29 *L*(**r**) maps and CPs in fluoride adducts of **CSSSe** (top) and **CSSeS** (bottom). (3,+1) CPs (pink spheres) and (3,-1) CPs (dark green spheres) are depicted around Ch2, Ch3 and F atoms. Bond critical points are small light green spheres.

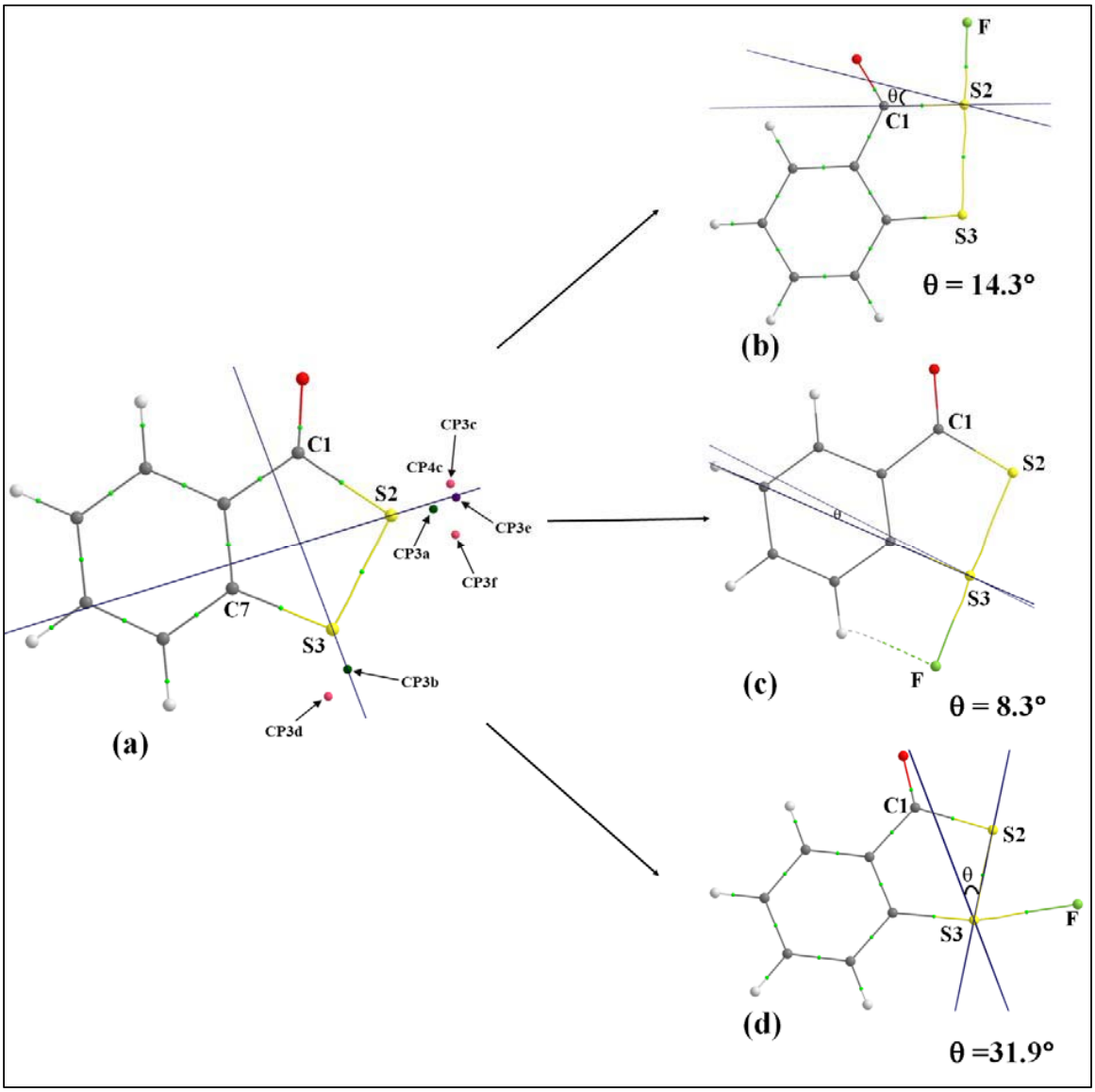

Figure S30 (a) CC_{lp1}-S2-CC_{lp2} and CC_{lp1}-S3-CC_{lp2} planes in **COSS**. (b) Angle θ between the plane defined by C1, S2 and one CC_{lp}, and the plane containing S2 and its lone pairs CC_{lp1} and CC_{lp2}. (c) Angle θ between the plane C7, S3 and one CC_{lp}, and the plane containing S3 atom and its lone pairs CC_{lp1} and CC_{lp2}. (d) Angle θ between the plane S2, S3 and one CC_{lp} (along the S2-S3 bond) and the plane containing S3 and its lone pairs CC_{lp1} and CC_{lp2}.

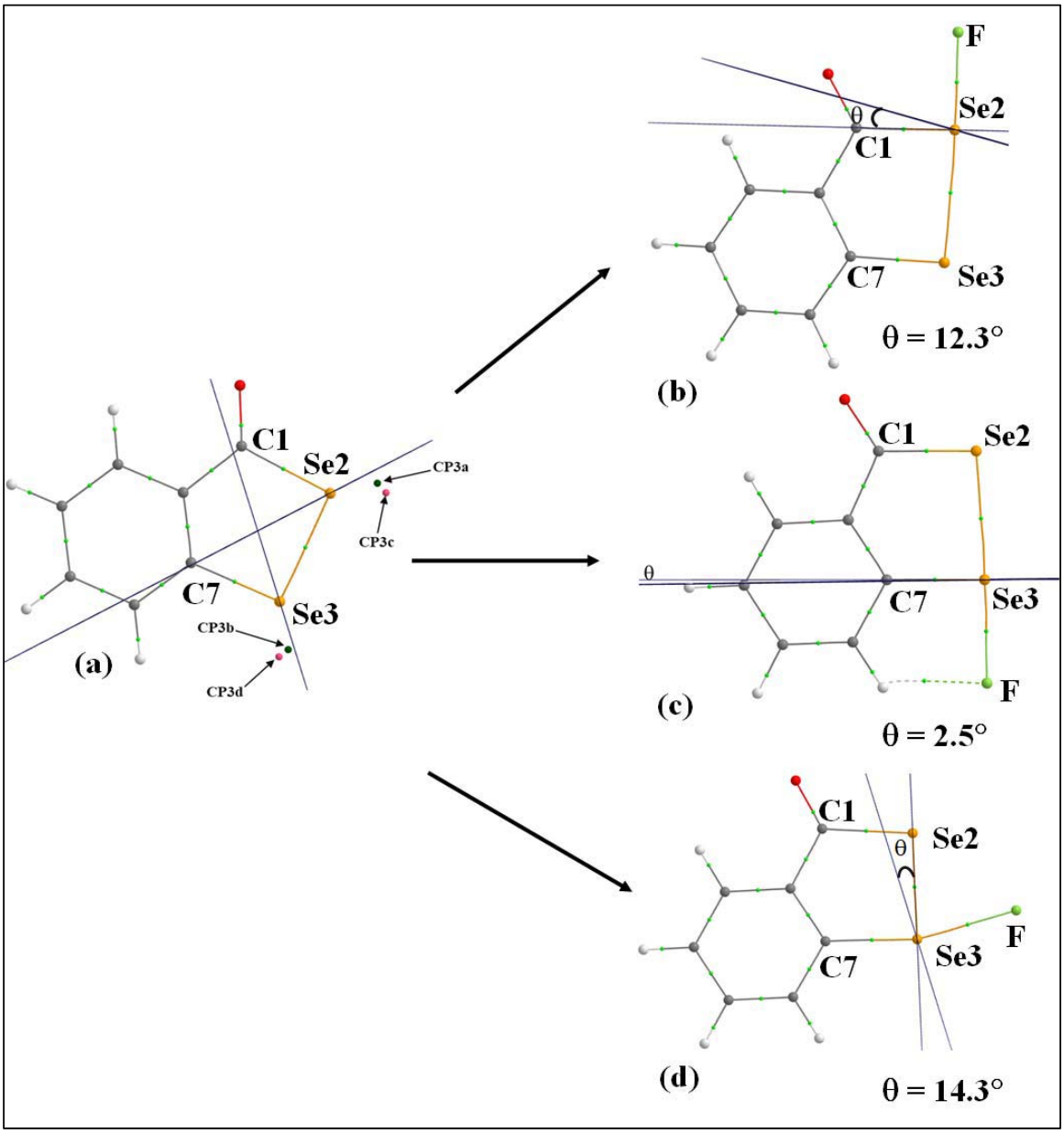

Figure S31 (a) CC_{lp1}-Se2-CC_{lp2} and CC_{lp1}-Se3-CC_{lp2} planes in **COSeSe**. (b) Angle θ between the plane defined by C1, Se2 and one CC_{lp}, and the plane containing Se2 and its lone pairs CC_{lp1} and CC_{lp2}. (c) Angle θ between the plane C7, Se3 and one CC_{lp}, and the plane containing Se3 atom and its lone pairs CC_{lp1} and CC_{lp2}. (d) Angle θ between the plane Se2, Se3 and one CC_{lp} (along the Se2-Se3 bond) and the plane containing S3 and its lone pairs CC_{lp1} and CC_{lp2}.

Table S1. Molecular Centroid-Centroid Distances for π-Stacking Motifs Observed in **COSS**, **COSeS** and **COSeSe** Isostructural Compounds.

π-stacking motif	**COSS**	**COSeS**	**COSeSe**
AA	3.612 Å	3.603 Å	3.643 Å
BB	3.707 Å	3.770 Å	3.875 Å
AB	3.829 Å	3.833 Å	3.896 Å

*The molecular centroid was calculated utilizing the non-hydrogen atoms present in the molecule.

Table S2. Selected intermolecular interaction observed in the crystal structure of **COSS**, **COSeS** and **COSeSe**.

Intermolecular Interaction	***d* (Å)**	**∠ (°)**	**Symmetry**
COSS			
C6A-H6A···S3B	3.05	128.2	x,-1+y,z
S2A-S3A···S3B	3.837	148.6	
C6A-H6A···O1B	2.46	133.8	2-x,2-y,2-z
C3B-H3B···S3A	3.26	140.6	
C5B-H5B···O1B	2.56	129.2	x,1.5-y,0.5+z
C3B-H3B···O1B	2.93	134.7	2-x,2-y,2-z
C1B-S2B···S2A	3.984	160.7	1-x,-0.5+y,1.5-z
C7B-S3B···S2A	3.830	162.1	
C5B-H5B···S3A	3.25	127.6	x,1.5-y,0.5+z
C6B-H6B···O1A	2.32	152.6	1-x,1-y,2-z
C3A-H3A···S3B	3.19	154.8	
C1A-S2A···O1A	3.199	162.7	1-x,0.5+y,1.5-z
C7A-S3A···O1A	3.081	165.1	
S3A-S2A···S3A	3.701	165.1	
C4A-H4A···S2A	2.94	144.6	x,1.5-y,0.5+z
C4A-H4A···S2B	3.01	130.5	x,1.5-y,-0.5+z
C4B-H4B···C5B(π)	2.96	159.5	2-x,0.5+y,2.5-z
COSeS			
C6A-H6A···S3Ba	2.82	136.6	-x,-1-y,-z
Se2Aa-S3Aa···S3Ba	3.887	150.8	
C6A-H6A···O1Ba	2.48	121.1	x,y,z
C3B-H3B···S3Aa	3.30	131.7	
C5B-H5B···O1Ba	2.48	130.0	x,-0.5-y,0.5+z

C3B-H3B···O1Ba	2.74	137.4	-x,-y,-z
C1Ba-Se2Ba···Se2Aa	3.909	156.1	1+x,-0.5-y,0.5+z
C7B-S3Ba···Se2Aa	3.773	160.9	
C5B-H5B···S3Aa	3.14	125.6	-x,-0.5+y,0.5-z
C6B-H6B···O1Aa	2.27	154.0	-1+x,-1+y,z
C3A-H3A···S3Ba	3.24	150.1	
C1A-Se2Aa···O1Aa	3.096	158.0	1-x,-0.5+y,0.5-z
C7A-S3Aa···O1Aa	3.029	163.6	
S3A-Se2Aa···S3Aa	3.517	164.1	
C4A-H4A···Se2Aa	2.92	139.2	x,0.5-y,-0.5+z
C4A-H4A···Se2Ba	2.95	131.7	-x,0.5+y,-0.5-z
C4B-H4B···C6B(π)	2.91	161.5	-x,0.5+y,0.5-z
COSeSe			
C6A-H6A···Se3B	3.07	125.7	x,-1+y,z
Se2A-Se3A···Se3B	3.819	147.1	
C6A-H6A···O1B	2.44	136.4	-x,-y,2-z
C3B-H3B···Se3A	3.21	134.9	
C5B-H5B···O1B	2.55	134.4	x,0.5-y,-0.5+z
C3B-H3B···O1B	3.02	135.1	-x,-y,2-z
C1B-Se2B···Se2A	3.925	157.7	1-x,0.5+y,2.5-z
C7B-Se3B···Se2A	3.769	159.8	
C5B-H5B···Se3A	3.28	123.0	x,0.5-y,-0.5+z
C6B-H6B···O1A	2.44	156.1	
C3A-H3A···Se3B	3.14	157.2	1-x,1-y,2-z
C1A-Se2A···O1A	3.292	155.8	1-x,0.5+y,2.5-z
C7A-Se3A···O1A	3.125	160.8	
Se3A-Se2A···Se3A	3.596	165.8	
C4A-H4A···Se2A	2.98	142.8	x,0.5-y,-0.5+z
C4A-H4A···Se2B	3.06	130.3	x,0.5-y,-0.5+z
C4B-H4B···C6B(π)	2.95	159.3	-x,-0.5+y,1.5-z

Table S3. Molecular Centroid-Centroid Distances for the two unique π-Stacking Motifs Observed in **CSSS**, **COSSe** and **CSSSe**.

π-stacking motif	**COSSe**	**CSSS**	**CSSSe**
AA1	3.730 Å	3.879 Å	3.889 Å
AA2	3.728 Å	3.991 Å	4.008 Å

Table S4. Selected intermolecular interaction in the crystal structures of **CSSS**, **COSSe** and **CSSSe**

Intermolecular Interaction	*d* (Å)	∠ (°)	Symmetry
CSSS (AYOZAR)			
C1-S2···S1	3.376	170.7	1.5-x,0.5+y,1.5-z
C7-S3···S1	3.428	164.1	
S3-S2···S3	3.955	164.4	
C4-H4···S2	3.04	140.0	x,-y,0.5+z
C6-H6···S1	3.01	132.3	0.5+x,-0.5+y,z
S2-S3···S1	3.373	151.2	
C5-H5···S2	3.03	158.4	0.5+x,0.5-y,0.5+z
COSSe			
C1-S2···O1 C7-Se3···O1	3.605 3.543	162.9 158.3	0.5-x,0.5+y,0.5-z
Se3-S2···Se3	3.783	167.8	
C4-H4···S2	2.84	144.6	x,1-y,0.5+z
C6-H6···O1	2.97	127.8	0.5+x,0.5+y,z
S2-Se3···O1	3.201	154.0	
C5-H5···S2	2.90	155.3	x,1-y,0.5+z
C7-Se3···Se3-C7	3.658	146.9	-x,y,0.5-z
CSSSe			
C1-S2···S1	3.471	169.4	1.5-x,0.5+y,0.5-z
C7-Se3···S1	3.456	161.0	
Se3-S2···Se3	3.910	164.4	
C4-H4···S2	3.07	140.8	x,-y,0.5+z
C6-H6···S1	3.03	131.1	0.5+x,-0.5+y,z
S2-Se3···S1	3.396	151.8	
C5-H5···S2	3.06	158.2	0.5+x,0.5-y,0.5+z
C7-Se3···Se3-C7	4.073	139.4	1-x,y,0.5-z

Table S5. Selected intermolecular interaction observed in the crystal structure of **CSSS** (AYOZAR01)

Intermolecular Interaction	*d* (Å)	∠ (°)	Symmetry
C4-H4···S1	3.38	132.9	-0.5-x,0.5+y,0.5-z
C3-H3···S2	2.75	148.2	
C5-H5···S1	3.04	133.6	-0.5+x,1.5-y,0.5+z
C6-H6···S1	2.87	126.1	0.5+x,1.5-y,0.5+z
C7-S3···S1	3.555	163.1	0.5-x,-0.5+y,0.5-z
C1-S2···S1	3.503	167.4	
S2-S3···S3	3.764	158.1	1-x,1-y,1-z
C6-H6···S3	3.15	142.4	

Table S6. Selected intermolecular interaction observed in the crystal structure of **CSSeS**

Intermolecular Interaction	***d* (Å)**	**∠ (°)**	**Symmetry**
C6A-H6A···S3A	3.16	150.9	-x,-1-y,-z
C4A-H4A···S1A	3.39	140.1	1-x,-y,-z
C3B-H3B···C5A	2.71	136.6	1-x,-y,-z
C1A-Se2A···S1B	3.346	171.8	-1+x,y,z
C7A-S3A···S1B	3.808	153.8	
C1B-Se2B···Se2A	3.763	154.9	1-x,-0.5+y,0.5-z
C7B-S3B···Se2A	3.525	164.8	
C1A-Se2A···S3B	3.573	163.8	1-x,0.5+y,0.5-z
Se2B-S3B···S1A	3.913	152.9	
S3B-Se2B···Se2B	3.518	164.4	2-x,0.5+y,0.5-z

Table S7. Structural characteristics of the ChB interactions in **COSeS, COSSe, CSSSe** and **CSSeS**

Compound	Motif	Interaction	σ-hole	*d* (Å)	RR	ζ_1 (°)	ζ_2 (°)	ρ (e/Å^3)	$\nabla^2\rho$ (e/Å^5)	|V|/G
COSeS	**I**	C7A/Se2Aa-S3Aa•••O1A-C1Aa	R2	3.029	0.91	163.6/70.6	110.1	0.082	1.02	0.79
		C1Aa/S3Aa-Se2Aa•••O1A-C1Aa	R2	3.096	0.91	158.0/67.3	114.7	0.073	0.92	0.80
		C1Aa/S3Aa-Se2Aa•••S3Aa-C7A/Se2Aa	R1A	3.516	0.95	77.3/164.1	125.9/94.5	0.061	0.56	0.82
	II	C7A/Se2Aa-S3Aa•••S3Ba-C7B/Se2Ba	R1B	3.887	1.08	87.8/150.8	144.3/103.7	0.027	0.29	0.66
	III	C7B/Se2Ba-S3Ba•••Se2Aa-C1Aa/S3Aa	R2	3.773	1.02	160.9/76.8	127.0/131.0	0.037	0.41	0.98
		C1Ba/S3Ba-Se2Ba•••Se2Aa-C1Aa/S3Aa	R2	3.909	1.03	156.1/70.00	110.6/112.9	0.039	0.36	0.77
COSSe	**I**	C1/Se3-S2•••O1=C1	R2	3.605	1.09	162.9/70.6	110.2	-	-	-
		C7/S2-Se3•••O1=C1	R2	3.543	1.04	158.3/73.7	110.2	0.032	0.37	0.76
		C1/Se3-S2•••Se3-C7/S2	R1A	3.783	1.02	87.7/167.8	124.6/86.0	0.040	0.38	0.74
	II	C7/S2-Se3•••O1=C1	R1B	3.201	0.94	97.8/154.0	150.4	0.056	0.73	0.76
CSSSe	**I**	C1/Se3-S2•••S1=C1	R2	3.471	0.94	169.4/71.1	101.5	0.063	0.64	0.75
		C7/S2-Se3•••S1=C1	R2	3.456	0.93	161.0/71.9	106.7	0.070	0.69	0.77
		C1/Se3-S2•••Se3-C7/S2	R1A	3.910	1.06	88.7/164.4	129.4/80.3	-	-	-
	II	C7/S2-Se3•••S1=C1	R1B	3.396	0.92	96.5/151.8	148.2	0.064	0.68	0.70
CSSeS	**I**	C1A/S3A-Se2A•••S1B=C1B	R2	3.346	0.90	171.8/84.0	134.0	0.082	0.79	0.87
		C7A/Se2A-S3A•••S1B=C1B	R2	3.808	1.06	153.8/60.9	132.5	-	-	-
	II	C1B/S3B-Se2B•••Se2A-C1A/S3A	R2	3.763	0.99	154.9/66.6	121.3/117.1	-	-	-
		C7B/Se2B-S3B•••Se2A-C1A/S3A	R2	3.525	0.95	164.8/78.5	87.1/118.4	0.066	0.63	0.84
	III	C1A/S3A-Se2A•••S3B-C7B/Se2B	R1a	3.573	0.97	163.8/100.6	124.7/106.4	0.067	0.63	0.84
		C7B/Se2B-S3B•••S1A=C1A	R1b	3.913	1.09	105.7/152.9	93.8	0.029	0.31	0.69
	IV	C1B/S3B-Se2B•••Se2B-C1B/S3B	R1a	3.518	0.93	99.4/164.4	83.9/118.4	0.077	0.60	0.91

Table S8: Topological parameters ρ, $\nabla^2\rho$ and |V|/G obtained at BCPs of the covalent bonds of **COSS**, **COSeSe**, **CSSS** and **CSSeSe**.

	COSS			**COSeSe**			**CSSS**			**CSSeSe**		
	ρ	$\nabla^2\rho$	|V|/G	ρ	$\nabla^2\rho$	|V|/G	ρ	$\nabla^2\rho$	|V|/G	ρ	$\nabla^2\rho$	|V|/G
Ch2-Ch3	0.95	-2.65	2.60	0.68	-0.82	2.26	0.93	-2.45	2.56	0.67	-0.72	2.23
Ch2-C1	1.20	-5.48	3.04	0.96	-2.53	2.53	1.38	-8.28	3.30	1.09	-3.47	2.55
Ch3-C7	1.35	-8.32	3.40	1.07	-3.39	2.56	1.36	-8.51	3.42	1.07	-3.48	2.57
Ch1-C1	2.89	-7.54	2.11	2.90	-6.15	2.09	1.53	-4.77	2.21	1.54	-5.18	2.23
C1-C2	1.90	-19.67	4.69	1.87	-18.97	4.64	1.94	-20.34	4.60	1.92	-19.91	4.58
C2-C3	2.13	-24.76	4.51	2.12	-24.37	4.49	2.12	-24.59	4.55	2.11	-24.08	4.53
C3-C4	2.22	-26.73	4.48	2.23	-26.83	4.49	2.23	-26.92	4.48	2.24	-27.05	4.48
C4-C5	2.14	-25.04	4.58	2.15	-25.28	4.59	2.14	-25.06	4.59	2.15	-25.30	4.60
C5-C6	2.20	-26.19	4.46	2.20	-26.19	4.47	2.21	-26.34	4.46	2.21	-26.37	4.47
C6-C7	2.14	-24.84	4.43	2.15	-24.86	4.42	2.14	-24.85	4.43	2.15	-24.89	4.43
C7-C2	2.16	-25.12	4.43	2.15	-24.81	4.41	2.12	-24.16	4.43	2.10	-23.72	4.41
C3-H3	2.00	-28.95	9.95	2.01	-28.98	9.95	2.01	-29.02	10.03	2.01	-29.05	9.99
C4-H4	1.99	-28.55	9.26	1.99	-28.53	9.26	1.99	-28.57	9.29	1.99	-28.54	9.27
C5-H5	1.99	-28.65	9.48	1.99	-28.62	9.45	2.00	-28.66	9.48	1.99	-28.63	9.45
C6-H6	1.99	-28.42	9.23	1.99	-28.37	9.19	1.99	-28.43	9.22	1.99	-28.37	9.17

*ρ in e/Å^3, $\nabla^2\rho$ in e/Å^5, |V|/G is dimensionless

Table S9 Topological parameters ρ, $\nabla^2\rho$ and |V|/G obtained at BCPs of the covalent bonds of **COSSe**, **COSeS**, **CSSSe** and **CSSeS**

	COSSe			**COSeS**			**CSSSe**			**CSSeS**		
	ρ	$\nabla^2\rho$	|V|/G	ρ	$\nabla^2\rho$	|V|/G	ρ	$\nabla^2\rho$	|V|/G	ρ	$\nabla^2\rho$	|V|/G
Ch2-Ch3	0.79	-1.34	2.35	0.79	-1.29	2.32	0.77	-1.19	2.31	0.78	-1.22	2.31
Ch2-C1	1.21	-5.62	3.05	0.95	-2.53	2.54	1.38	-8.35	3.29	1.09	-3.57	2.58
Ch3-C7	1.07	-3.53	2.59	1.34	-8.17	3.37	1.09	-3.62	2.59	1.35	-8.28	3.38
Ch1-C1	2.89	-7.65	2.12	2.91	-6.05	2.09	1.53	-5.32	2.25	1.54	-4.72	2.21
C1-C2	1.88	-19.20	4.70	1.89	-19.42	4.63	1.92	-19.99	4.62	1.93	-20.22	4.57
C2-C3	2.13	-24.68	4.50	2.12	-24.46	4.50	2.12	-24.43	4.54	2.11	-24.23	4.54
C3-C4	2.22	-26.71	4.49	2.23	-26.85	4.48	2.23	-26.93	4.49	2.24	-27.06	4.48
C4-C5	2.15	-25.23	4.58	2.15	-25.11	4.59	2.15	-25.24	4.59	2.14	-25.13	4.60
C5-C6	2.20	-26.07	4.47	2.21	-26.31	4.46	2.20	-26.26	4.47	2.21	-26.47	4.46
C6-C7	2.15	-24.98	4.42	2.14	-24.70	4.44	2.15	-24.99	4.42	2.14	-24.74	4.44
C7-C2	2.16	-25.09	4.41	2.15	-24.79	4.43	2.12	-24.06	4.41	2.10	-23.77	4.43
C3-H3	2.00	-28.96	9.97	2.00	-28.96	9.93	2.01	-29.03	10.03	2.01	-29.04	9.99
C4-H4	1.99	-28.55	9.27	1.99	-28.52	9.24	1.99	-28.57	9.30	1.99	-28.54	9.27
C5-H5	1.99	-28.63	9.46	1.99	-28.64	9.47	1.99	-28.64	9.46	1.99	-28.65	9.47
C6-H6	1.99	-28.38	9.19	1.99	-28.41	9.23	1.99	-28.39	9.18	1.99	-28.41	9.21

*ρ in e/Å^3, $\nabla^2\rho$ in e/Å^5, |V|/G is dimensionless

Table S10. QTAIM charge (in *e*) on the atoms present in the molecules.

	COSS	**COSSe**	**COSeS**	**COSeSe**	**CSSS**	**CSSSe**	**CSSeS**	**CSSeSe**
Ch1	-1.13	-1.13	-1.13	-1.13	0.14	0.14	0.16	0.16
Ch2	0.02	-0.08	0.20	0.09	0.15	0.05	0.35	0.24
Ch3	0.08	0.28	-0.03	0.17	0.08	0.27	-0.04	0.16
C1	0.96	0.96	0.90	0.90	-0.46	-0.45	-0.55	-0.55
C2	0.02	0.01	0.01	0.01	0.04	0.04	0.04	0.04
C3	0.01	0.01	0.01	0.01	0.01	0.01	0.01	0.01
C4	0.01	0.01	0.01	0.01	0.01	0.01	0.01	0.01
C5	0.00	0.00	0.00	0.00	0.00	0.00	0.00	0.00
C6	0.02	0.03	0.02	0.02	0.02	0.02	0.02	0.02
C7	-0.16	-0.24	-0.15	-0.23	-0.16	-0.24	-0.15	-0.24
H3	0.07	0.07	0.06	0.07	0.07	0.07	0.06	0.07
H4	0.03	0.03	0.03	0.03	0.03	0.03	0.03	0.03
H5	0.03	0.03	0.03	0.03	0.03	0.03	0.03	0.03
H6	0.04	0.03	0.04	0.03	0.04	0.03	0.03	0.03

Table S11. Nucleophilic Power (L/ρ in $Å^{-2}$) of Charge Concentration (CC) Sites in the Electron Valence Shell of Chalcogen Atoms in Gas Phase Molecules

	CC_1	**CC_2**	**CC_3**	**CC_4**	**CC_5**	**CC_4**
COSS	15.90	16.43	9.24	9.24	9.74	9.74
COSSe	15.96	16.49	9.12	9.12	0.69	0.69
COSeS	15.77	16.37	0.23	0.23	9.57	9.57
COSeSe	15.83	16.42	0.16	0.16	0.57	0.57
CSSS	8.93	9.16	9.35	9.35	9.57	9.57
CSSSe	8.91	9.16	9.20	9.20	0.52	0.52
CSSeS	8.95	9.19	0.25	0.25	9.42	9.42
CSSeSe	8.93	9.18	0.16	0.16	0.42	0.42

Table S12 Angle ∠CC_{lp1}-Chal-CC_{lp2} (°) for the chalcogen atoms in the molecules.

Molecule	∠CC_1-Chal1-CC_2	∠CC_3-Chal2-CC_4	∠CC_5-Chal3-CC_6
COSS	136.5	134.5	133.1
COSSe	136.9	135.0	145.6
COSeS	134.5	149.9	133.5
COSeSe	134.8	150.0	145.7
CSSS	149.8	127.1	132.1
CSSSe	149.5	127.4	145.5
CSSeS	148.9	144.8	132.6
CSSeSe	148.7	145.1	145.6

Table S13 Selected angles ∠Ch3-Ch2-CP, ∠Ch2-Ch3-CP, ∠C1-Ch2-CP and ∠C7-Ch3-CP involving the CPs of L(**r**)

Angles (°)	COSS	COSSe	COSeS	COSeSe	CSSS	CSSSe	CSSeS	CSSeSe
∠Ch3-Ch2-CP1a	154.7	153.3	127.9	128.7	154.3	153.2	129.9	130.6
∠Ch2-Ch3-CP1b	152.4	127.8	151.3	128.7	151.0	126.9	149.6	127.5
∠C1-Ch2-CP2a	149.0	152.3	-		151.6	154.6		-
∠C7-Ch3-CP2b	151.8	-	155.5		151.2		155.0	-
∠Ch3-Ch2-CP3a	125.7	129.0	119.2	127.0	128.0	130.6	129.4	135.4
∠C1-Ch2-CP3a	137.3	133.5	148.4	139.9	133.9	130.8	136.8	130.1
∠Ch2-Ch3-CP3b	132.2	139.1	135.2	145.0	133.9	143.9	137.2	149.0
∠C7-Ch3-CP3b	133.0	130.4	129.4	123.7	132.9	127.1	129.2	121.5
∠Ch3-Ch2-CP3c	145.1	149.5	106.8	115.5	148.6	150.3	142.9	148.2
∠C1-Ch2-CP3c	117.9	113.1	160.7	151.4	113.3	111.1	123.3	117.3
∠Ch2-Ch3-CP3d	156.6	151.9	157.9	155.8	159.4	156.3	160.5	159.5
∠C7-Ch3-CP3d	108.6	117.5	106.7	112.9	107.4	114.7	105.9	111.1
∠Ch3-Ch2-CP3e	132.7	126.1	-	-	120.9	-	-	-
∠C1-Ch2-CP3e	130.4	136.5	-	-	141.0	-	-	-
∠Ch3-Ch2-CP3f	100.6	104.3	-	-	107.8	-	-	-
∠C1-Ch2-CP3f	162.5	158.3	-	-	154.0	-	-	-
∠C1-Ch2-CP4a	129.9	129.3	124.2	124.1	130.0	129.8	125.0	124.9
∠C7-Ch3-CP4a	127.1	122.1	127.0	122.1	126.4	120.9	125.7	120.6
∠C1-Ch2-CP4b	139.5	147.0	-	-	143.1	149.7	-	-
∠C7-Ch3-CP4b	124.1	117.9	-	-	122.0	115.8	-	-
∠C1-Ch2-CP4c	126.0	-	119.7	-	127.1	-	121.1	-
∠C7-Ch3-CP4c	141.1	-	148.8	-	138.7	-	147.2	-

Table S14. Electrophilic Power (L/ρ in $Å^{-2}$) of Charge Depletion (CD) Sites in the Electron Valence Shell of Chalcogen Atoms in Gas Phase Molecules

	Type	**COSSE**			**COSES**			**CSSSE**			**CSSES**		
		$\nabla^2\rho$ ($e/Å^5$)	ρ ($e/Å^3$)	L/ρ ($Å^{-2}$)	$\nabla^2\rho$ ($e/Å^5$)	ρ ($e/Å^3$)	L/ρ ($Å^{-2}$)	$\nabla^2\rho$ ($e/Å^5$)	ρ ($e/Å^3$)	L/ρ ($Å^{-2}$)	$\nabla^2\rho$ ($e/Å^5$)	ρ ($e/Å^3$)	L/ρ ($Å^{-2}$)
CP1a	(3,+1)	-0.22	0.82	0.27	2.63	0.33	-7.97	0.51	0.80	-0.64	2.97	0.38	-7.81
CP1b	(3,+1)	2.62	0.35	-7.48	-0.09	0.83	0.11	2.62	0.36	-7.28	-0.35	0.84	0.42
CP2a	(3,+1)	-2.23	0.89	2.50				-1.73	0.87	1.99			
CP2b	(3,+1)				-1.68	0.87	1.93				-1.92	0.88	2.18
CP3a	(3,-1)	-8.58	1.16	7.40	1.37	0.60	-2.28	-9.21	1.18	7.80	1.33	0.62	-2.14
CP3b	(3,-1)	1.54	0.57	-2.70	-8.29	1.15	9.53	1.92	0.56	-3.43	-8.26	1.15	7.18
CP3c	(3,+1)	1.64	0.33	-4.97	1.56	0.36	-4.33	1.63	0.32	-5.09	1.59	0.36	-4.42
CP3d	(3,+1)	1.63	0.38	-4.29	1.62	0.32	-5.06	1.61	0.38	-4.24	1.61	0.32	-5.03
CP3e	(3,+3)	1.65	0.34	-4.85									
CP3f	(3,+1)	1.64	0.33	-4.97									
CP4a	(3,+1)	1.93	0.33	-5.84	1.94	0.33	-5.88	1.92	0.32	-6.00	1.94	0.32	-6.06
CP4b	(3,+3)	2.17	0.36	-6.03				2.29	0.36	-6.36			
CP4c	(3,+3)				2.28	0.36	-6.33				2.24	0.36	-6.22

Table S15. Structural and topological characteristics of the ChB interactions in **COSeS, COSSe, CSSSe** and **CSSeS**

Compound	Motif	Interaction	σ-hole	RR	*d* (Å)	ρ (e/Å^3)	$\nabla^2\rho$ (e/Å^5)	|V|/G	CD	(L/ρ)$_{CC}$ (e/Å^{-2})	(L/ρ)$_{CD}$ (e/Å^{-2})	Δ(L/ρ) (e/Å^{-2})	dcc…cd	Δ(L/ρ)/ ($d_{CC...CD}$)^2	α(°)
COSeS	**I**	S3Aa•••O1A	R2	0.91	3.029	0.082	1.02	0.79	CP2b/	16.3	1.65/	14.7/	2.00/	3.67	5.7/
		Se2Aa•••O1A	R2	0.91	3.096	0.073	0.92	0.80	CP3c/		-4.46/	20.81/	2.84/	2.58	27.4/
									CP3d/		-4.97	21.32/	2.85/	2.62	21.1/
									CP4a/		-6.49/	22.84/	1.89/	6.39	5.7/
									CP4c		-6.80	23.15	1.76	7.47	9.9
		Se2Aa•••S3Aa	R1A	0.95	3.516	0.061	0.56	0.82	CP1a/	9.57	-8.02/	17.59/	2.26/	3.44	11.2/
									CP3c		-4.32	13.89	2.92	1.63	16.9
	II	S3Aa•••S3Ba	R1B	1.08	3.887	0.027	0.29	0.66	CP1b/	9.58	0.06/	9.52/	2.82/	1.20	4.4/
									CP3d		-5.02	14.6	2.53	2.28	12.8
	III	S3Ba•••Se2Aa	R2	1.02	3.773	0.037	0.41	0.98	CP2b/	0.26	1.86/	-1.60/	2.55/	-0.24	11.2/
		Se2Ba•••Se2Aa	R2	1.03	3.909	0.039	0.36	0.77	CP3c/	(CC1)	-4.43/	4.69/	2.30/	0.89	13.6/
									CP3d/		-4.99/	5.25/	3.50/	0.43	30.2/
									CP4a/		-6.08/	6.34/	2.29/	1.21	12.0/
									CP4c		-6.33	6.59	2.28	1.27	24.2
									CP2b/	0.19	1.86/	-1.67/	3.42/	-0.14	19.3/
									CP3d		-4.99	5.18	3.76	0.37	2.6
									(CC2)						
COSSe	**I**	S2•••O1	R2	1.09	3.605	-	-	-	CP2a/	16.38	2.32/	14.06/	2.68/	1.96	2.6/
		Se3•••O1	R2	1.04	3.543	0.032	0.37	0.76	CP3c/		-4.98/	21.36/	3.44/	1.80	22.3/
									CP3d/		-4.36/	20.74/	3.21/	2.01	18.5/
									CP4a/		-6.19/	22.57/	2.43/	3.82	5.7/
									CP4b		-6.18	22.56	2.41	3.88	14.5
		S2•••Se3	R1A	1.02	3.783	0.040	0.38	0.74	CP1a/	0.68	0.13/	0.55/	2.51/	0.09	18.7/
									CP3c		-5.10	5.78	1.98	1.47	2.6
	II	Se3•••O1	R1B	0.94	3.201	0.056	0.73	0.76	CP1b/	16.46	-7.46/	23.92/	2.84/	2.96	13.8/
									CP3d	(CC1)	-4.53	20.99	2.48	3.41	15.6
									CP1b/	15.91	-7.46/	23.37/	2.75/	3.09	6.3/
									CP3d	(CC2)	-4.53	20.44	2.82	2.57	25.6
CSSSe	**I**	S2•••S1	R2	0.94	3.471	0.063	0.64	0.75	CP2a/	9.18	1.78/	7.4/	2.33/	1.36	8.1/
		Se3•••S1	R2	0.93	3.456	0.070	0.69	0.77	CP3c/		-5.00/	14.18/	3.25/	1.34	29.5/
									CP3d/		-4.31/	13.49/	2.88/	1.63	19.3/
									CP4a/		-6.54/	15.72/	2.02/	3.85	9.9/
									CP4b		-6.65	15.83	2.05	3.77	22.8
		S2•••Se3	R1A	1.06	3.910	-	-	-	CP1a/	0.54	-0.60/	1.14/	2.75/	0.15	19.8/
									CP3c		-5.08	5.62	2.18	1.18	4.4
	II	Se3•••S1	R1B	0.92	3.396	0.064	0.68	0.70	CP1b/	9.18	-7.31/	16.49/	3.09/	1.73	18.9/
									CP3d	(CC1)	-4.48	13.66	2.29	2.60	16.7
									CP1b/		-7.31/	16.23/	2.84/	2.01	10.6/
									CP3d	8.92	-4.48	13.4	2.70	1.84	24.8
										(CC2)					
CSSeS	**I**	Se2A•••S1B	R2	0.90	3.346	0.082	0.79	0.87	CP2b/	8.94	2.07/	6.87/	2.75/	0.91	12.3/
		S3A•••S1B	R2	1.06	3.808	-	-	-	CP3c/	(CC1)	-4.49/	13.43/	3.38/	1.33	30.3/
									CP3d/		-4.92/	13.86/	3.62/	1.06	8.5/
									CP4a/		-6.19/	15.13/	2.56/	2.32	10.9/
									CP4c		-6.37	15.25	2.49	2.46	4.4
										9.20					
									CP3c	(CC2)	-4.49	13.69	2.69	1.89	9.9
	II	Se2B•••Se2A	R2	0.99	3.763	-	-	-	CP2b/	0.37	1.94/	-1.57/	1.99/	-0.40	2.6/
		S3B•••Se2A	R2	0.95	3.525	0.066	0.63	0.84	CP3c/		-4.47/	4.84/	3.04/	0.52	27.1/
									CP3d/		-5.00/	5.37/	2.80/	0.68	27.9/
									CP4a/		-6.40/	6.77/	1.93/	1.82	4.4/
									CP4c		-6.43	6.80	1.78	2.15	9.6
	III	Se2A•••S3B	R1a	0.97	3.575	0.067	0.63	0.84	CP1a/	9.41	-7.87/	17.28/	2.64/	2.48	9.9/
									CP3c		-4.49	13.9	2.45	2.31	21.1
		S3B•••S1A	R1b	1.09	3.916	0.029	0.31	0.69	CP1b/	9.19	0.23/	8.96/	2.80/	1.14	8.1/
									CP3d		-5.19	14.38	2.20	2.97	7.3
	IV	Se2B•••Se2B	R1a	0.93	3.518	0.077	0.60	0.91	CP1a/	0.09	-7.75/	7.84/	2.23/	1.58	4.4/
									CP3c		-4.54	4.63	1.70	1.60	19.4

Table S16. Geometrical parameters for [**CCh1Ch2Ch3** + F]$^{-1}$ complexes formed in region R1A.

	d (Å) (Ch2···F)	∠(°) Ch3-Ch2···F	*d(Å)* (Ch2-Ch3)	Δ*d(Å)* (Ch2-Ch3)	*d(Å)* (C1-Ch2)	Δ*d(Å)* (C1-Ch2)	*d(Å)* (C7-Ch3)	Δ*d(Å)* (C7-Ch3)
[**COSS**+F]$^{-1}$	1.82	179.0	2.44	+0.35	1.83	+0.00	1.73	-0.03
[**COSSe**+F]$^{-1}$	1.82	178.1	2.57	+0.34	1.83	+0.01	1.88	-0.03
[**COSeS**+F]$^{-1}$	1.94	176.5	2.52	+0.29	1.98	-0.01	1.74	-0.02
[**COSeSe**+F]$^{-1}$	1.94	177.3	2.64	+0.28	1.98	0.00	1.89	-0.02
[**CSSS**+F]$^{-1}$	1.81	173.8	2.41	+0.30	1.78	+0.03	1.72	-0.04
[**CSSSe**+F]$^{-1}$	1.82	172.2	2.55	+0.30	1.78	+0.03	1.88	-0.02
[**CSSeS**+F]$^{-1}$	1.93	178.3	2.49	+0.25	1.93	+0.03	1.73	-0.03
[**CSSeSe**+F]$^{-1}$	1.94	177.0	2.61	+0.24	1.93	+0.03	1.88	-0.03

*Δ*d* corresponds to the difference in the bond length observed between complex and monomer, i.e. Δ*d* = *d* (complex) – *d* (monomer).

Table S17. Geometrical parameters for [**CCh1Ch2Ch3** + F]$^{-1}$ complexes formed in region R1B.

	d (Å) (Ch3···F)	∠(°) Ch2-Ch3···F	*d(Å)* (Ch2-Ch3)	Δ*d(Å)* (Ch2-Ch3)	*d(Å)* (C1-Ch2)	Δ*d(Å)* (C1-Ch2)	*d(Å)* (C7-Ch3)	Δ*d(Å)* (C7-Ch3)
[**COSS**+F]$^{-1}$	1.98	178.4	2.30	+0.21	1.76	-0.07	1.77	+0.01
[**COSSe**+F]$^{-1}$	2.03	176.2	2.44	+0.21	1.76	-0.06	1.92	+0.01
[**COSeS**+F]$^{-1}$	2.01	176.8	2.42	+0.19	1.92	-0.07	1.78	+0.02
[**COSeSe**+F]$^{-1}$	2.05	177.6	2.55	+0.19	1.92	-0.06	1.93	+0.02
[**CSSS**+F]$^{-1}$	1.98	178.7	2.26	+0.15	1.72	-0.03	1.77	+0.01
[**CSSSe**+F]$^{-1}$	2.03	175.9	2.41	+0.16	1.72	-0.03	1.92	+0.02
[**CSSeS**+F]$^{-1}$	2.02	177.2	2.38	+0.14	1.87	-0.03	1.77	+0.01
[**CSSeSe**+F]$^{-1}$	2.05	177.2	2.52	+0.15	1.87	-0.03	1.92	+0.03

*Δ*d* corresponds to the difference in the bond length observed between complex and monomer, i.e. Δ*d* = *d* (complex) – *d* (monomer).

Table S18 Geometrical parameters for [**CCh1Ch2Ch3** + F]$^{-1}$ complexes in region R2.

	d (Å) (Ch2···F)	∠(°) Ch3-Ch2···F	*d (Å)* (Ch3···F)	∠(°) Ch2-Ch3···F	*d(Å)* (Ch2-Ch3)	Δ*d(Å)* (Ch2-Ch3)	*d(Å)* (C1-Ch2)	Δ*d(Å)* (C1-Ch2)	*d(Å)* (C7-Ch3)	Δ*d(Å)* (C7-Ch3)
[**COSS**+F]$^{-1}$	2.57	155.6	2.25	165.2	2.09	0.00	1.79	-0.04	1.78	+0.02
[**COSSe**+F]$^{-1}$	2.79	150.4	2.16	164.8	2.25	+0.02	1.78	-0.04	1.96	+0.05
[**COSeS**+F]$^{-1}$	2.23	163.1	2.67	150.6	2.24	+0.01	1.97	-0.02	1.75	-0.01
[**COSeSe**+F]$^{-1}$	2.83	145.6	2.20	164.4	2.36	+0.00	1.94	-0.04	1.96	+0.05
[**CSSS**+F]$^{-1}$	2.51	157.4	2.25	162.6	2.08	-0.03	1.73	-0.02	1.77	+0.01
[**CSSSe**+F]$^{-1}$	2.74	151.7	2.16	163.1	2.24	-0.01	1.73	-0.02	1.95	+0.05
[**CSSeS**+F]$^{-1}$	2.18	164.3	2.67	148.4	2.25	+0.01	1.92	+0.02	1.74	-0.02
[**CSSeSe**+F]$^{-1}$	2.75	147.9	2.21	161.5	2.34	-0.03	1.88	-0.02	1.95	+0.04

*Δ*d* corresponds to the difference in the bond length observed between complex and monomer, i.e. Δ*d* = *d* (complex) – *d* (monomer).

Table S19. Topological parameters at BCPs of selected bonds in [**CCh1Ch2Ch3** + F]$^{-1}$ complexes formed via region R1A. Values in *italic* correspond to topological parameters at BCPs for monomers.

	ρ (e/Å^3)	$\nabla^2\rho$ (e/Å^5)	|V|/G
[**COSS**+F]$^{-1}$			
Ch2···F	0.89	0.89	1.90
Ch2-Ch3	0.49 *0.95*	1.00 *-2.65*	1.65 *2.60*
C1-Ch2	1.23 *1.20*	-6.05 *-5.48*	3.16 *3.04*
C7-Ch3	1.40 *1.35*	-9.33 *-8.32*	3.25 *3.40*
[**COSSe**+F]$^{-1}$			
Ch2···F	0.89	1.03	1.88
Ch2-Ch3	0.42 *0.79*	0.95 *-1.34*	1.59 *2.35*
C1-Ch2	1.23 *1.21*	-5.97 *-5.62*	3.15 *3.05*
C7-Ch3	1.09 *1.07*	-2.51 *-3.53*	2.32 *2.59*
[**COSeS**+F]$^{-1}$			
Ch2···F	0.73	5.07	1.47
Ch2-Ch3	0.45 *0.79*	1.01 *-1.29*	1.64 *2.32*
C1-Ch2	0.98 *0.95*	-2.92 *-2.53*	2.61 *2.54*
C7-Ch3	1.38 *1.34*	-9.05 *-8.17*	3.24 *3.37*
[**COSeSe**+F]$^{-1}$			
Ch2···F	0.73	5.00	1.47
Ch2-Ch3	0.40 *0.68*	0.88 *-0.82*	1.60 *2.26*
C1-Ch2	0.98 *0.96*	-2.83 *-2.53*	2.59 *2.53*
C7-Ch3	1.08 *1.07*	-2.52 *-3.39*	2.33 *2.56*

[**CSSS**+F]$^{-1}$			
Ch2···F	0.90	0.92	1.90
Ch2-Ch3	0.51 *0.93*	0.97 *-2.45*	1.68 *2.56*
C1-Ch2	1.32 *1.38*	-7.45 *-8.28*	3.25 *3.30*
C7-Ch3	1.42 *1.36*	-9.66 *-8.51*	3.28 *3.42*
[**CSSSe**+F]$^{-1}$			
Ch2···F	0.90	1.16	1.87
Ch2-Ch3	0.44 *0.77*	0.95 *-1.19*	1.61 *2.31*
C1-Ch2	1.32 *1.38*	-7.38 *-8.35*	3.23 *3.29*
C7-Ch3	1.11 *1.09*	-2.70 *-3.62*	2.34 *2.59*
[**CSSeS**+F]$^{-1}$			
Ch2···F	0.75	5.12	1.48
Ch2-Ch3	0.48 *0.78*	0.98 *-1.22*	1.67 *2.31*
C1-Ch2	1.04 *1.09*	-3.20 *-3.57*	2.56 *2.58*
C7-Ch3	1.40 *1.35*	-9.33 *-8.28*	3.28 *3.38*
[**CSSeSe**+F]$^{-1}$			
Ch2···F	0.74	5.04	1.48
Ch2-Ch3	0.42 *0.67*	0.87 *-0.72*	1.63 *2.23*
C1-Ch2	1.04 *1.09*	-3.08 *-3.47*	2.54 *2.55*
C7-Ch3	1.10 *1.07*	-2.72 *-3.48*	2.36 *2.57*

Table S20. Topological parameters at BCPs of selected bonds in [**CCh1Ch2Ch3** + F]$^{-1}$ complexes formed via region R1B. Values in *italic* correspond to topological parameters at BCPs for monomers.

	ρ (e/Å^3)	$\nabla^2\rho$ (e/Å^5)	|V|/G
[**COSS**+F]$^{-1}$			
Ch3···F	0.63	3.69	1.44
Ch2-Ch3	0.64 *0.95*	0.13 *-2.65*	1.96 *2.60*
C1-Ch2	1.34 *1.20*	-7.80 *-5.48*	3.20 *3.04*
C7-Ch3	1.32 *1.35*	-8.07 *-8.32*	3.41 *3.40*
[**COSSe**+F]$^{-1}$			
Ch3···F	0.60	4.54	1.38
Ch2-Ch3	0.52 *0.79*	0.62 *-1.34*	1.80 *2.35*
C1-Ch2	1.33 *1.21*	-7.74 *-5.62*	3.19 *3.05*
C7-Ch3	1.06 *1.07*	-3.55 *-3.53*	2.60 *2.59*
[**COSeS**+F]$^{-1}$			
Ch3···F	0.59	3.96	1.37
Ch2-Ch3	0.58 *0.79*	0.26 *-1.29*	1.91 *2.32*
C1-Ch2	1.05 *0.95*	-2.93 *-2.53*	2.47 *2.54*
C7-Ch3	1.32 *1.34*	-7.79 *-8.17*	3.37 *3.37*
[**COSeSe**+F]$^{-1}$			
Ch3···F	0.58	4.46	1.36
Ch2-Ch3	0.48 *0.68*	0.53 *-0.82*	1.79 *2.26*
C1-Ch2	1.04 *0.96*	-2.80 *-2.53*	2.45 *2.53*
C7-Ch3	1.05 *1.07*	-3.38 *-3.39*	2.58 *2.56*

[**CSSS**+F]$^{-1}$			
Ch3···F	0.63	3.78	1.43
Ch2-Ch3	0.69 *0.93*	-0.12 *-2.45*	2.03 *2.56*
C1-Ch2	1.45 *1.38*	-9.89 *-8.28*	3.31 *3.30*
C7-Ch3	1.34 *1.36*	-8.28 *-8.51*	3.43 *3.42*
[**CSSSe**+F]$^{-1}$			
Ch3···F	0.60	4.56	1.37
Ch2-Ch3	0.56 *0.77*	0.52 *-1.19*	1.84 *2.31*
C1-Ch2	1.44 *1.38*	-9.73 *-8.35*	3.28 *3.29*
C7-Ch3	1.07 *1.09*	-3.66 *-3.62*	2.61 *2.59*
[**CSSeS**+F]$^{-1}$			
Ch3···F	0.59	4.05	1.36
Ch2-Ch3	0.61 *0.78*	0.08 *-1.22*	1.97 *2.31*
C1-Ch2	1.14 *1.09*	-3.26 *-3.57*	2.43 *2.58*
C7-Ch3	1.33 *1.35*	-7.95 *-8.28*	3.38 *3.38*
[**CSSeSe**+F]$^{-1}$			
Ch2···F	0.58	4.46	1.35
Ch2-Ch3	0.49 *0.67*	0.53 *-0.72*	1.79 *2.23*
C1-Ch2	1.04 *1.09*	-2.50 *-3.47*	2.45 *2.55*
C7-Ch3	1.05 *1.07*	-3.38 *-3.48*	2.58 *2.57*

Table S21. Topological parameters at BCPs of selected bonds in [**CCh1Ch2Ch3** + F]$^{-1}$ complexes formed via region R2. Values in *italic* correspond to topological parameters at BCPs for monomers.

	ρ (e/Å^3)	$\nabla^2\rho$ (e/Å^5)	|V|/G
[**COSS**+F]$^{-1}$			
Ch2···F	-	-	-
Ch3···F	0.35	3.80	1.07
Ch2-Ch3	0.98 *0.95*	-3.21 *-2.65*	2.75 *2.60*
C1-Ch2	1.32 *1.20*	-7.42 *-5.48*	3.25 *3.04*
C7-Ch3	1.33 *1.35*	-8.08 *-8.32*	3.26 *3.40*
[**COSSe**+F]$^{-1}$			
Ch2···F	-	-	-
Ch3···F	0.46	4.22	1.21
Ch2-Ch3	0.78 *0.79*	-1.43 *-1.34*	2.38 *2.35*
C1-Ch2	1.32 *1.21*	-7.39 *-5.62*	3.24 *3.05*
C7-Ch3	0.97 *1.07*	-1.87 *-3.53*	2.29 *2.59*
[**COSeS**+F]$^{-1}$			
Ch2···F	0.40	3.93	1.15
Ch3···F	-	-	-
Ch2-Ch3	0.79 *0.79*	-1.39 *-1.29*	2.36 *2.32*
C1-Ch2	0.99 *0.95*	-2.42 *-2.53*	2.41 *2.54*
C7-Ch3	1.37 *1.34*	-8.88 *-8.17*	3.36 *3.37*
[**COSeSe**+F]$^{-1}$			
Ch2···F	-	-	-
Ch3···F	0.43	4.07	1.17
Ch2-Ch3	0.69 *0.68*	-1.12 *-0.82*	2.36 *2.26*
C1-Ch2	1.03 *0.96*	-3.02 *-2.53*	2.53 *2.53*
C7-Ch3	0.97	-1.84	2.29

	1.07	*-3.39*	*2.56*
[**CSSS**+F]$^{-1}$			
Ch2···F	-	-	-
Ch3···F	0.35	3.84	1.07
Ch2-Ch3	1.00 *0.93*	-3.39 *-2.45*	2.77 *2.56*
C1-Ch2	1.44 *1.38*	-9.66 *-8.28*	3.37 *3.30*
C7-Ch3	1.36 *1.36*	-8.60 *-8.51*	3.31 *3.42*
[**CSSSe**+F]$^{-1}$			
Ch2···F	-	-	-
Ch3···F	0.46	4.26	1.22
Ch2-Ch3	0.79 *0.77*	-1.53 *-1.19*	2.39 *2.31*
C1-Ch2	1.45 *1.38*	-9.73 *-8.35*	3.37 *3.29*
C7-Ch3	1.00 *1.09*	-2.06 *-3.62*	2.31 *2.59*
[**CSSeS**+F]$^{-1}$			
Ch2···F	0.44	4.17	1.19
Ch3···F	-	-	-
Ch2-Ch3	0.78 *0.78*	-1.33 *-1.22*	2.35 *2.31*
C1-Ch2	1.06 *1.09*	-2.41 *-3.57*	2.34 *2.58*
C7-Ch3	1.40 *1.35*	-9.35 *-8.28*	3.39 *3.38*
[**CSSeSe**+F]$^{-1}$			
Ch2···F	-	-	-
Ch3···F	0.41	4.04	1.16
Ch2-Ch3	0.72 *0.67*	-1.26 *-0.72*	2.39 *2.23*
C1-Ch2	1.13 *1.09*	-3.37 *-3.47*	2.46 *2.55*
C7-Ch3	1.00 *1.07*	-2.10 *-3.48*	2.32 *2.57*

Table S22. Topological parameters at the BCP of the C-H…F interaction in region R1B.

	ρ (e/Å^3)	$\nabla^2\rho$ (e/Å^5)	|V|/G
[**COSS**+F]$^{-1}$	0.15	2.49	0.82
[**COSSe**+F]$^{-1}$	0.13	2.10	0.80
[**COSeS**+F]$^{-1}$	0.17	2.67	0.83
[**COSeSe**+F]$^{-1}$	0.15	2.30	0.81
[**CSSS**+F]$^{-1}$	0.16	2.53	0.82
[**CSSSe**+F]$^{-1}$	0.14	2.17	0.81
[**CSSeS**+F]$^{-1}$	0.17	2.71	0.83
[**CSSeSe**+F]$^{-1}$	0.15	2.36	0.82

References

[1] Lamberts, K.; Handels, P.; Englert, U.; Aubert, E., Espinosa, E. Stabilization of polyiodide chains via anion···anion interactions: experiment and theory. *CrystEngComm* **2016**, *18*, 3832−3841.

[2] Bader, R. F. W. Atoms in Molecules − A Quantum Theory; Clarendon: Oxford, *1990*

[3] Brezgunova, M.; Lieffrig, J.; Aubert, E.; Dahaoui, S. ; Fertey, P. ; Lebègue, S.; Angyan,J. ; Fourmigué, M. ; Espinosa E. Chalcogen Bonding: Experimental and Theoretical Determinations from Electron Density Analysis – Geometrical Preferences Driven by Electrophilic-Nucleophilic Interactions. *Cryst. Growth Design* **2013**, *13*, 3283−3289.

[4] Brezgunova, M. E.; Aubert, E.; Lieffrig, J.; Dahaoui, S.; Fertey, P.; Lebègue, S.; Jelsch, C.; Ángyán, J. G.; Espinosa, E. Charge Density Analysis and Topological Properties of Hal(3)-Synthons and Their Comparison with Competing Hydrogen Bonds. *Cryst. Growth Des*. **2012,** *12*, 11, 5373−5386.